NASA / CR-2002-212132

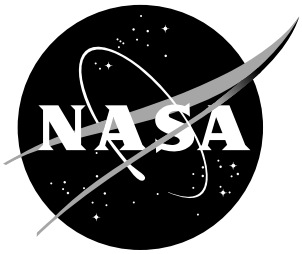

Energy Absorbing Seat System for an Agricultural Aircraft

Sotiris Kellas
Lockheed Martin Engineering and Sciences Company, Hampton, Virginia

December 2002

The NASA STI Program Office ... in Profile

Since its founding, NASA has been dedicated to the advancement of aeronautics and space science. The NASA Scientific and Technical Information (STI) Program Office plays a key part in helping NASA maintain this important role.

The NASA STI Program Office is operated by Langley Research Center, the lead center for NASA's scientific and technical information. The NASA STI Program Office provides access to the NASA STI Database, the largest collection of aeronautical and space science STI in the world. The Program Office is also NASA's institutional mechanism for disseminating the results of its research and development activities. These results are published by NASA in the NASA STI Report Series, which includes the following report types:

- TECHNICAL PUBLICATION. Reports of completed research or a major significant phase of research that present the results of NASA programs and include extensive data or theoretical analysis. Includes compilations of significant scientific and technical data and information deemed to be of continuing reference value. NASA counterpart of peer-reviewed formal professional papers, but having less stringent limitations on manuscript length and extent of graphic presentations.

- TECHNICAL MEMORANDUM. Scientific and technical findings that are preliminary or of specialized interest, e.g., quick release reports, working papers, and bibliographies that contain minimal annotation. Does not contain extensive analysis.

- CONTRACTOR REPORT. Scientific and technical findings by NASA-sponsored contractors and grantees.

- CONFERENCE PUBLICATION. Collected papers from scientific and technical conferences, symposia, seminars, or other meetings sponsored or co-sponsored by NASA.

- SPECIAL PUBLICATION. Scientific, technical, or historical information from NASA programs, projects, and missions, often concerned with subjects having substantial public interest.

- TECHNICAL TRANSLATION. English-language translations of foreign scientific and technical material pertinent to NASA's mission.

Specialized services that complement the STI Program Office's diverse offerings include creating custom thesauri, building customized databases, organizing and publishing research results ... even providing videos.

For more information about the NASA STI Program Office, see the following:

- Access the NASA STI Program Home Page at ***http://www.sti.nasa.gov***

- E-mail your question via the Internet to help@sti.nasa.gov

- Fax your question to the NASA STI Help Desk at (301) 621-0134

- Phone the NASA STI Help Desk at (301) 621-0390

- Write to:
  NASA STI Help Desk
  NASA Center for AeroSpace Information
  7121 Standard Drive
  Hanover, MD 21076-1320

NASA / CR-2002-212132

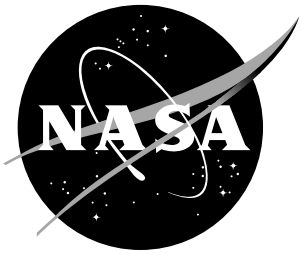

Energy Absorbing Seat System for an Agricultural Aircraft

Sotiris Kellas
Lockheed Martin Engineering and Sciences Company, Hampton, Virginia

National Aeronautics and
Space Administration

Langley Research Center
Hampton, Virginia 23681-2199

Prepared for Langley Research Center
under Contract NAS1-96014

December 2002

The use of trademarks or names of manufacturers in the report is for accurate reporting and does not constitute an official endorsement, either expressed or implied, of such products or manufacturers by the National Aeronautics and Space Administration.

Available from:

NASA Center for AeroSpace Information (CASI)
7121 Standard Drive
Hanover, MD 21076-1320
(301) 621-0390

National Technical Information Service (NTIS)
5285 Port Royal Road
Springfield, VA 22161-2171
(703) 605-6000

Energy Absorbing Seat System

for an Agricultural Aircraft

Sotiris Kellas
Lockheed Martin Engineering And Sciences Co.

ABSTRACT

A task was initiated to improve the energy absorption capability of an existing aircraft seat through cost-effective retrofitting, while keeping seat-weight increase to a minimum. This task was undertaken as an extension of NASA ongoing safety research and commitment to general aviation customer needs.

Only vertical crash scenarios have been considered in this task which required the energy absorbing system to protect the seat occupant in a range of crash speeds up to 31 ft/sec. It was anticipated that, the forward and/or side crash accelerations could be attenuated with the aid of airbags, the technology of which is currently available in automobiles and military helicopters.

Steps which were followed include, preliminary crush load determination, conceptual design of cost effective energy absorbers, fabrication and testing (static and dynamic) of energy absorbers, system analysis, design and fabrication of dummy seat/rail assembly, dynamic testing of dummy seat/rail assembly, and finally, testing of actual modified seat system with a dummy occupant. A total of ten full scale tests have been performed including three of the actual aircraft seat. Results from full-scale tests indicated that occupant loads were attenuated successfully to survivable levels. In particular, the occupant maximum lumbar load was attenuated from 1936 lb., which resulted from a relatively mild velocity at impact of 25.7 ft/sec., down to 1500 lb., from a 32.5 ft./sec. test.

INTRODUCTION

During the initial formulation of the "Advanced General Aviation Transport Experiments", AGATE, program and in the spirit of addressing general aviation customer needs, a task was identified and initiated to provide improved energy absorption capability for an existing aircraft seat through cost-effective retrofitting. The seat is used in a single place agricultural aircraft of steel frame construction, designated the "Thrush" and built by the Ayres Corporation of Albany Georgia. The seat arrangement used in the plane provided a good opportunity for adding energy absorption. The feature that made the seat system particularly attractive are the two steel tubular rails which restrain transverse motion of the seat and provide three height adjustments. For this study one aircraft seat together with two sets of rails were provided by the aircraft manufacturer.

Several energy absorbing concepts were considered but only the ones that met the following criteria were chosen for testing. The design criteria were:

(a) provide vertical load attenuation to survivable levels (lumbar loads to equal or less than 1500 lb.) for vertical crash velocities up to 31 ft/sec.,
(b) maintain the three seat adjustment positions of the original seat, as well as the ease of adjustment,
(c) chosen concept could be applied to both existing and new aircraft with comparable cost and efficiency,
(d) energy could be absorbed in both the compressive and tensile stroke of the seat, and provide post crash integrity,
(e) keep the fabrication cost and weight of the energy absorbing system to a minimum,
(f) meet fail-safe requirement. That is, in case of system failure during a crash, the energy absorption capability would be at least as good as that of the original seat system's and,
(g) due to space constraints between the seat and the rear cockpit bulkhead, the energy absorbers could not extend more the 0.5" behind the top seat bracket.

Two energy absorbing concepts were selected according to the above criteria. The first concept could dissipate energy through friction, between the seat rails and a steel ring which was constrained by a shaft collar. This energy absorbing concept is referred to as the "constrained ring". In the second concept energy was absorbed mainly through the crushing of thin-wall aluminum tubes which were placed over the seat rails, being referred to as the "crush tube" concept. Both concepts were evaluated statically as well as dynamically, and one was chosen for further testing under full scale conditions.

Preliminary full scale testing of the seat system showed that binding of the seat and bending of the rails were major problems which had to be solved before crash energy could be absorbed through stroking of the seat. In order to preserve the only aircraft seat available, further preliminary full scale tests aimed at isolating and solving the seat binding problems were performed using a simulated seat which was custom build for this purpose. This had similar weight distribution to the aircraft seat plus occupant, and could accommodate the original seat brackets in the same way. During full scale tests, both the dummy seat and the actual aircraft seat were mounted on a custom build platform with the seat rails supported in a similar fashion to that in the actual plane.

Ten full scale tests, seven with the dummy seat and three with the actual aircraft seat were carried out using the 70 ft drop tower of the Impact Dynamic Research Facility. Impact velocities ranged from 25.7 to 32.5 ft/sec., with impact (deceleration) pulse magnitude in the range of 64 to 92 G. The deceleration pulse was produced when the platform and seat assembly were dropped into a steel box filled with fine glass beads.

In the first test, the actual seat (with a dummy occupant) was tested at a relatively mild impact velocity of 25.7 ft/s to obtain datum values for occupant loads. In tests two through eight the dummy seat was used to proof the energy absorbing concept and/or various modifications to the seat brackets and rails. The last two tests were carried out on the actual aircraft seat with the original seat rails and redesigned bottom seat bracket. The final test was carried out at an impact velocity of 32.5 ft/s which resulted in survivable occupant loads.

Results from preliminary as well as typical full scale tests are presented. The method of fabrication and installation of the shock absorbers on the seat are also discussed.

DESIGN AND TESTING OF ENERGY ABSORBERS

A schematic of the original seat assembly is shown in figure 1. Because the seat is free to ride along the rails, when the lock pins are removed, this seat system provided a good base for incorporating energy absorption cost effectively. By allowing the seat to stroke in a controlled manner, during a severe impact, crash loads could be attenuated to survivable levels. Possible obstacles to achieving survivable impacts at vertical velocities of 31 ft/sec. included:

(a) limited stroke. When the seat height was adjusted to the lowest position, the maximum possible stroke was approximately 7.0".
(b) seat binding. It was anticipated that due to the large moment arm between the seat brackets and the center of gravity, C.G., of the active weight, binding of the seat could take place, thus inhibiting stroking of the seat.

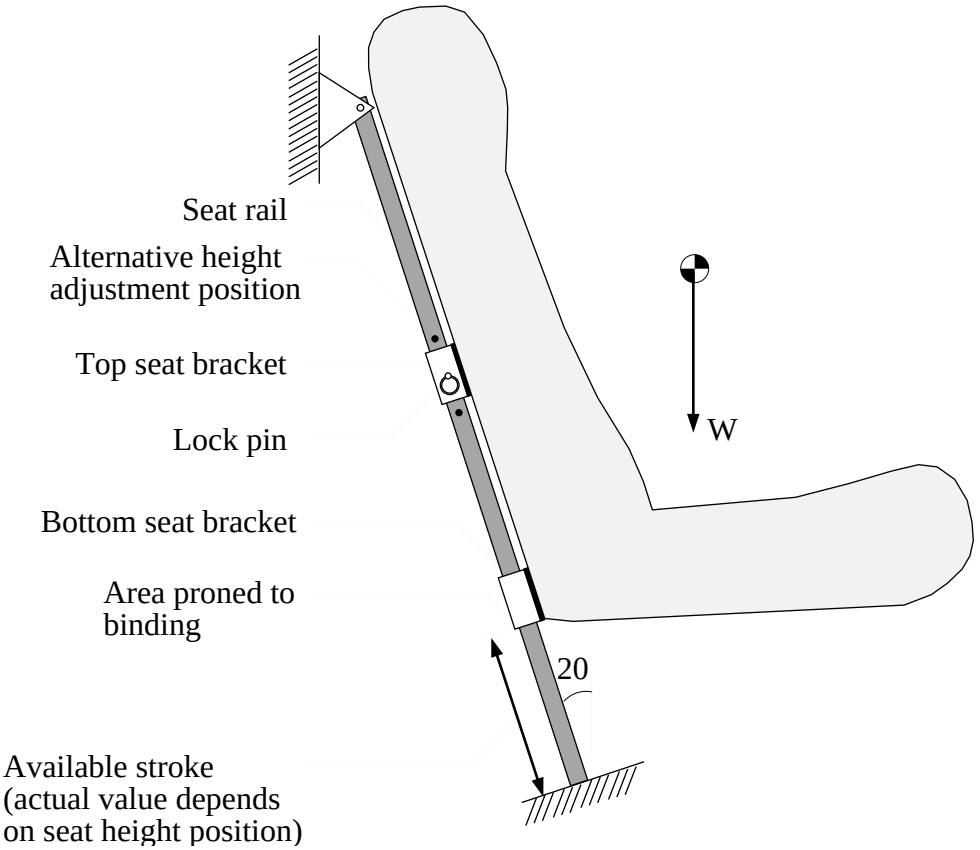

Fig.1 Schematic of original seat assembly. Note that, when the lock pin is removed the seat is free to ride along the rails.

Preliminary calculations indicated that at least 10.0" of stroke were needed in order to limit the seat accelerations, along the rail, to less than 19 G. For a stroke of 7.0" the seat accelerations, along the rail, would be approximately 26.5 G. In either case occupant loads would be survivable if the seat structure absorbed enough energy to limit the vertical lumbar loads to 1500 lb. or less. Calculations of the dynamic seat loading were based on equation 1 which was derived using the principle of conservation of energy and the assumptions that:

(a) the crash is purely vertical,
(b) the seat plus occupant mass remains rigid and uniform during crash and,
(c) the load sustained by the energy absorber during stroking of the seat is uniform.

$$G' = (H + S\cos(20°))/S \quad (1)$$

In equation 1, H is the vertical drop height (equal to approximately 15 ft. for 31 ft/sec. vertical impact velocity), S is the crush stroke (measured along the rail direction) and G (G' signifies the rail direction) is a dimensionless constant, multiple of the gravitational constant. The 20° angle represents the departure of the seat rail from the vertical.

The dynamic load in the range of 19 to 26G, along the rail direction, was chosen for the preliminary calculation of the crush load, based on the following two assumptions:

(a) the vertical load acting on the seat is equal to the weight of the occupant (minus weight of legs) plus the weight of the seat. For the 50 percentile male dummy the vertical active load was 158 lb., 24 lb. of which was contributed by the seat.
(b) the friction between the rails and the seat brackets was neglected.

Using the component of the active load along the rails and multiplying by the G' range, the crush load range was determined to be approximately 3300 ± 500 lb. Since some frictional resistance was anticipated during stroking of the seat the lower load limit was thought to be more appropriate.

With the preliminary crush load known, appropriate energy absorbing methods were considered. While a multitude of methods could be used to dissipate crash energy only two concepts met all of design requirements.

The first concept consisted of two off-the-shelf shaft collars which were machined to accommodate a steel split ring (spring) as shown in figure 2.

The collars were made of low carbon steel and had dimensions of 1.125" bore, 1.875" outer diameter, and 0.5" width. One collar was then inserted in each of the two top seat brackets, which had a slot machined to accommodate the collar, and over the seat rail. Crash energy was absorbed mainly through friction between the constrained 0.125" thick high-carbon steel ring and the steel rail. This concept was originally very attractive because of its simplicity, low weight, large stroke (almost 100%) and, the capability of tailoring the crushing load to any individual occupant weight.

Only two relatively minor modifications to the original seat assembly were required for this design. The first modification was carried out on the top seat brackets. A 0.5" wide slot was machined in each bracket to accommodate the shaft collar. To ensure adequate residual stiffness in the bracket a flange was welded to bridge the top and bottom halves, as shown in the inset of figure 2. Seat height adjustment was achieved by means of a "T" Allen wrench which was soldered onto the shaft-collar screw. With the shaft collar loosened the seat height could be adjusted to three positions, determined by the location of three shallow grooves on the seat rails. The three shallow (0.008" deep) grooves, which were plastically inserted in each rail, represent the second modification to the original seat system. A heavy duty pipe cutting tool with a modified cutting wheel was used to insert the grooves at the desired rail locations (original hole positions). Following dynamic testing this concept was rejected due to excessive load-rate sensitivity and high crush initiation load.

The second concept, which was eventually selected for full scale testing, consisted of two thin-wall aluminum tubes which could be placed over the rails and between the two seat brackets as shown in figure 3.

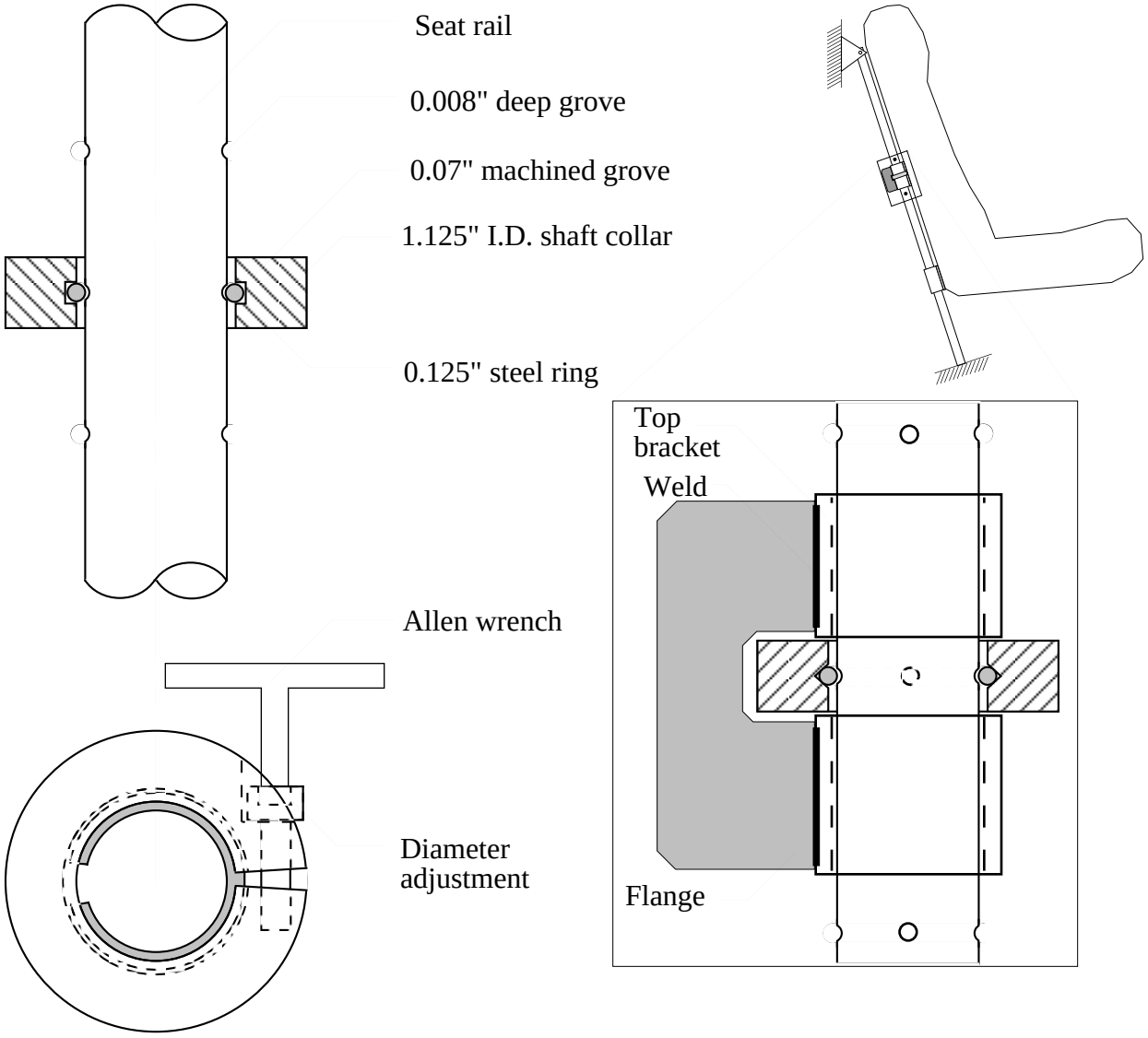

Fig.2 Constrained ring energy absorbing concept. Energy is absorbed through friction between the steel ring and the seat rail. The magnitude of the frictional force is determined by the depth of the seat rail grove and the diameter of the shaft collar.

Crash energy was dissipated through crushing of the tube over the seat rail. Since the seat rails inhibited global collapse of the tube, this concept was found to be reliable. Moreover, it was verified through dynamic testing that this concept was relatively load-rate insensitive. To eliminate the possibility of brittle fracture and ensure fully plastic deformations during crushing the 3003 aluminum alloy was selected with appropriate geometry to produce the desired sustained crushing load.

The average sustained crashing load, P_{av}, was calculated for several choices of off-the-shelf aluminum tubing using equation 2, reference [1].

$$P_{av} = 2(\pi t)^{1.5} r^{0.5} \sigma_y / 1.316 \qquad (2)$$

The tube that produced the closest crushing load to the desired range had a wall thickness, t, of 0.035", and outer diameter, 2r, of 1.25". The yield stress, σ_y, was assumed to be 30 ksi. The calculated crushing

load was 1300 lb. Two of these tubes, one for each rail, would produce at least 2600 lb. of crushing resistance. Note that, 2600 lb. was the least expected value since, in the actual application, the tubes would be crushed over an 1” diameter mandrel (the seat rail).

The total length of the tube was limited by the available stroke distance of the seat, and the distance between the top and bottom seat brackets. With the original bottom seat bracket in place the maximum length of the tube could not exceed 9”. All full scale tests were carried out with 9” long crush tubes. However, subsequent redesign of the bottom seat bracket, to eliminate binding, also provided additional space to possibly accommodate a longer crush tube, at least 10.5” long.

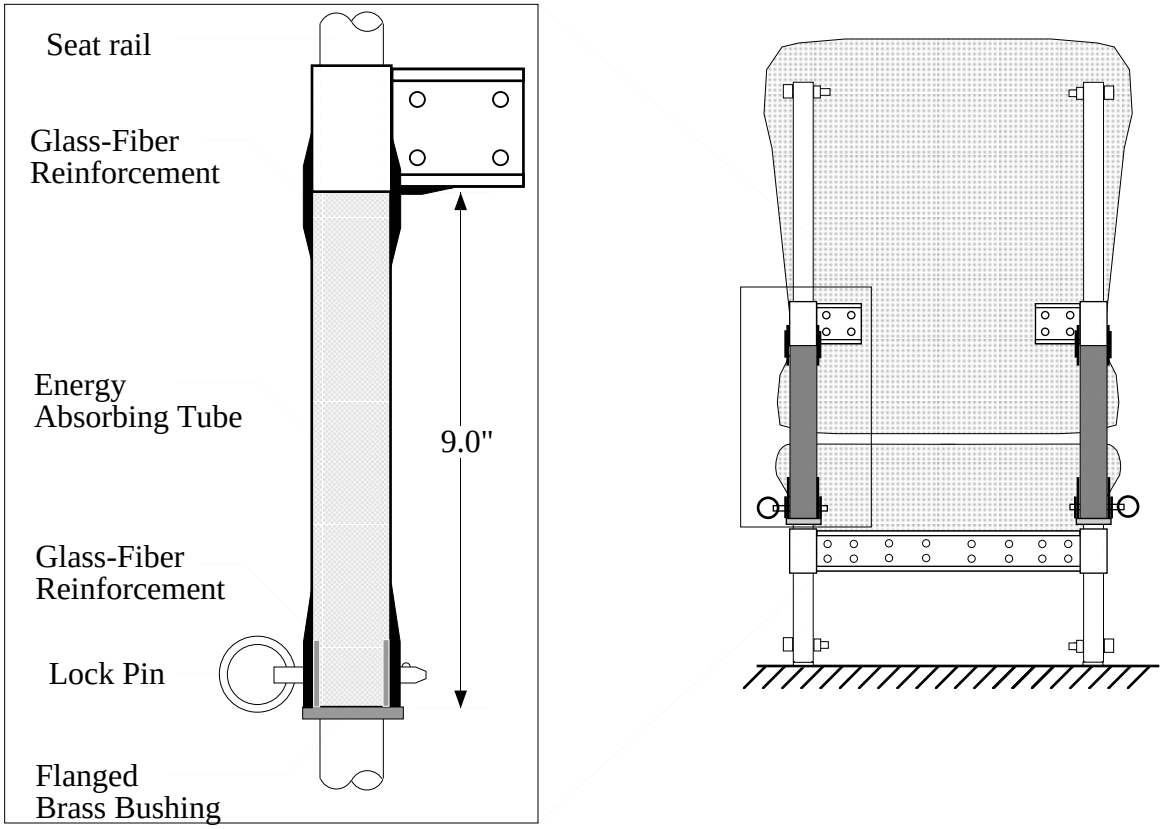

Fig.3 Crush tube energy absorbing concept. Energy is absorbed through the plastic deformation of the aluminum tube during the compressive stroke of the seat. Note that the lock pin, which in the original seat was located in the center of the top bracket, is now located on the bottom end of the crush tube.

The crush tubes were integrated into the seat system with glass reinforced fabric to couple one aluminum tube to the bottom of each top bracket. New pin holes were drilled in each rail to accommodate the height adjustment, and glass fiber reinforced fabric was used to strengthen the area around the pin as shown in figure 3. A flanged brass bushing was also inserted in the lower end of the tube to provide additional reinforcement as well as align the tube to the rail.

Static Tests

Static tests were carried out on a standard screw-driven load frame machine, typically at a displacement rate of 1”/min. These tests were used for preliminary evaluation of the maximum crash stroke capability of the energy absorbers, their crush initiation load, and their sustained crushing load (1650±250 lb. required per energy absorber, based on preliminary calculations). In the case of the “constrained ring”, static loading was also used to determined the appropriate torque (for each collar) needed to produce a given crushing load.

Typical set-ups for static crush testing for both energy absorbing concepts are shown schematically in figure 4, and typical load displacement responses for each concept are shown in figures 5 and 6 for the "constrained ring" and "crush tube" respectively.

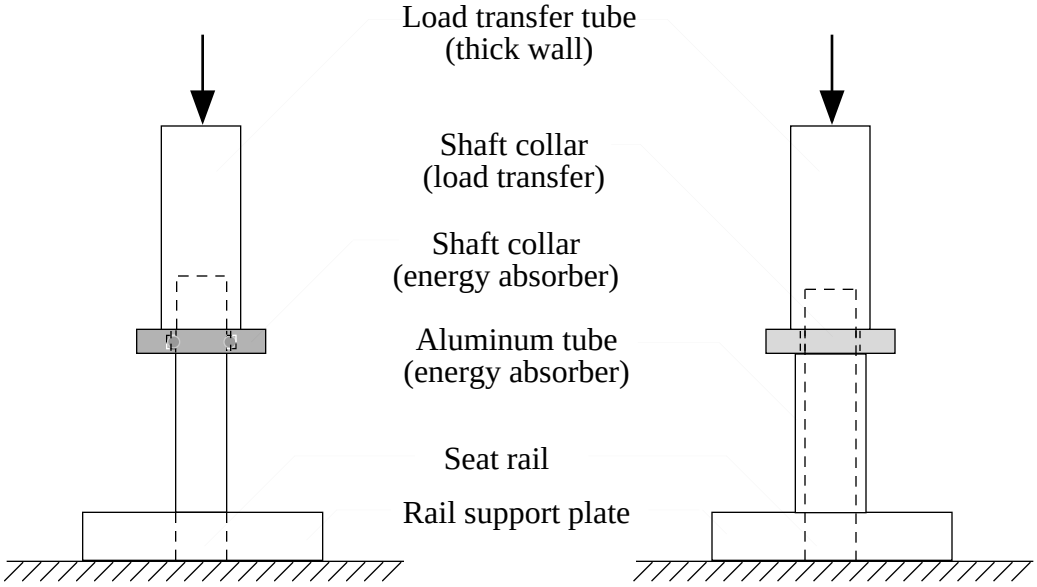

(a) "Constrained Ring" (b) "Crush Tube"

Fig.4 Schematic of static test set-up.

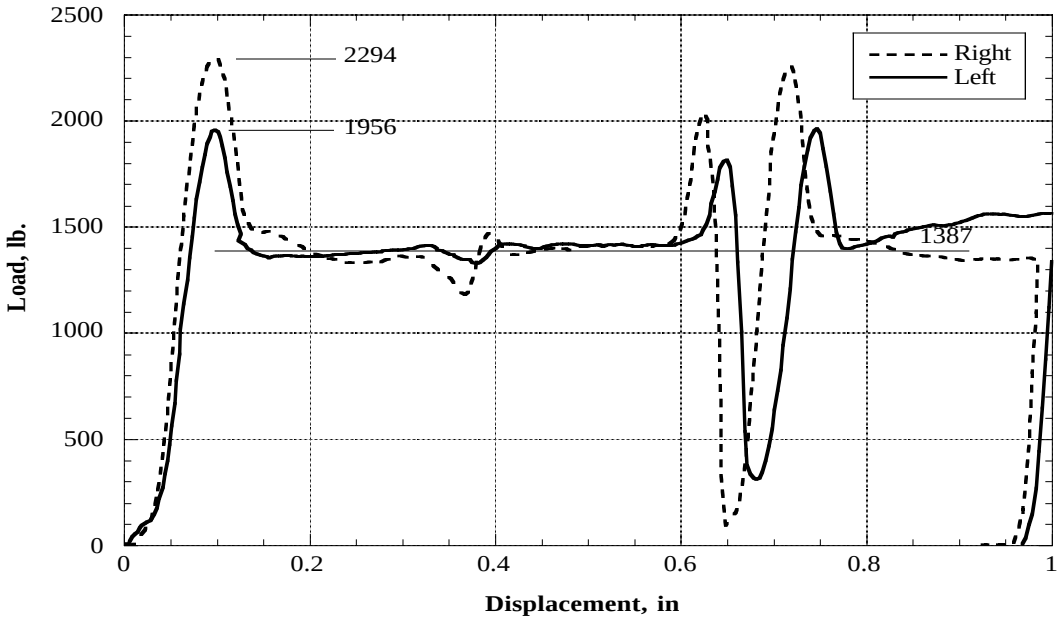

Fig.5 Static Load/Displacement responses of two constrained rings. Right and left refer to the left and right seat rails. The difference in the initiation load between the two rings could be attributed to a slight difference in rail grove depths.

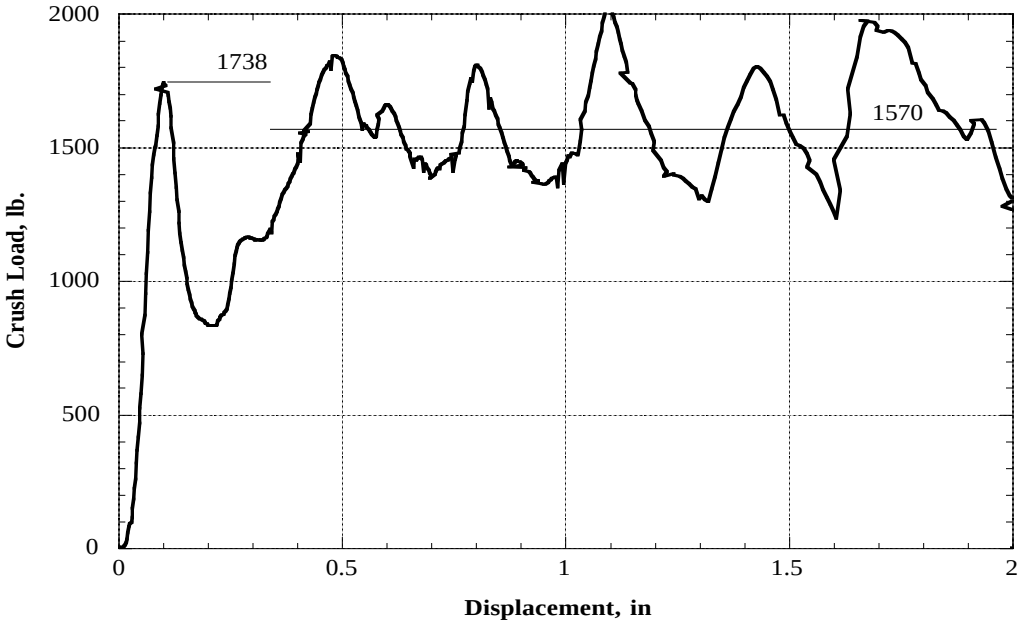

Fig.6 Static Load/Displacement response of aluminum crush tube.

Note that an undesirable feature in the constrained ring concept is the relatively high initiation load compared to the sustained crushing load. This is due to the fact that crashing cannot proceed until the constrained ring is forced out of the grove. With the grove eliminated, this peak would still exist (because the static coefficient of friction is always greater than its dynamic counterpart), but it would not be as pronounced. In any case, the groves in the rails were needed to define the three seat height positions and to ensure that a hand tightened collar could produce the desired ring constraint, needed for adequate sustained crush load.

A clear advantage that the constrained ring offered over the crush tube was the attainable stroke, which was almost 100% as compared to approximately 77% for the crush tube geometry used. Note that the stroke of the installed tube could actually be less than 77% depending on the way the tube is coupled to the seat.

Dynamic Tests

Dynamic component tests were carried out on a 14 ft. drop tower which was equipped with a hydraulic programmer capable of generating a sine pulse of adjustable magnitude and duration. Dynamic tests were carried out for the primary purpose of investigating the effect of loading rate on the crushing load. Therefore, these tests were essential in the final choice of the most appropriate energy absorber.

The dynamic test configuration is shown in figure 7 for both energy absorbing concepts. Two elements were tested simultaneously (in tandem) in order to simulate more closely the actual seat loading. The fixture used consisted of an impact mass, a reaction plate and four shafts The shafts were attached to the impact mass and were free to slide through the reaction plate. The reaction plate was fitted with brass bushings to minimize frictional losses. Two diagonal shafts were replaced by seat rail stock and the energy absorbers were placed over these rails as shown in figure 7. Stroking of the impact mass occurred when the reaction plate was decelerated by the pulse programmer. The impact mass was selected to correspond approximately to that of the active mass of the seat.

Dynamic data from two damped accelerometers were acquired at 10k samples/sec. per channel using a personal computer equipped with an analog to digital converter. After each drop data were processed with the aid of a custom data processing application and stored in the form of load and crush displacement. Processing, included filtering of the data, at typically 250 Hz, using a low pass “Chebyshev” filter routine.

A typical dynamic load crush-displacement response for the constrained ring concept is shown in figure 8.

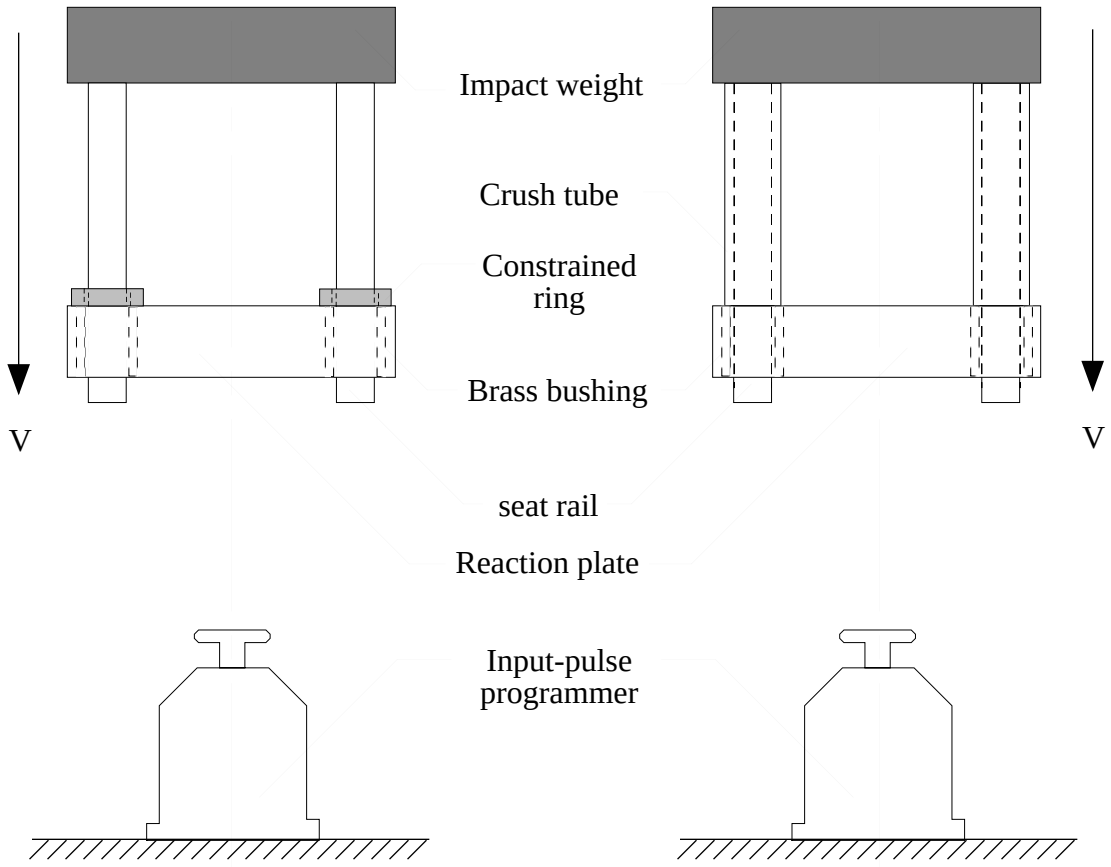

(a) Constrained Ring (b) Crush Tube

Fig.7 Schematic of dynamic test set-up.

An interesting feature in the dynamic response of the constrained ring concept, shown in figure 8, is the relatively large (3 times as large) initiation load compared to the sustained crushing load. However, in the static case the initiation load was on average only 1.5 times greater than the sustained load.

Comparing the static and dynamic loads, an increase in the initiation load of 12% was observed from static to the dynamic case, whereas a 44% reduction in the crushing load was observed from static to the dynamic case. Clearly, the increase in the loading rate from 1 in/min. to 20 ft/sec. had the greatest influence on the sustained crushing load.

Due to this relatively large load-rate dependency of the sustained crushing load, the constrained ring concept was found to be unacceptable. Therefore, all subsequent element and full scale investigations were concentrated solely on the crush tube concept.

A series of dynamic tests have been contacted on aluminum crush tubes with impact velocities ranging from 10 to 20 ft/sec.. In this series of tests, pieces of tubes were cut to predetermined lengths and tested as shown in figure 7b. A typical dynamic load crush-displacement response for the crush tube concept is presented in figure 9.

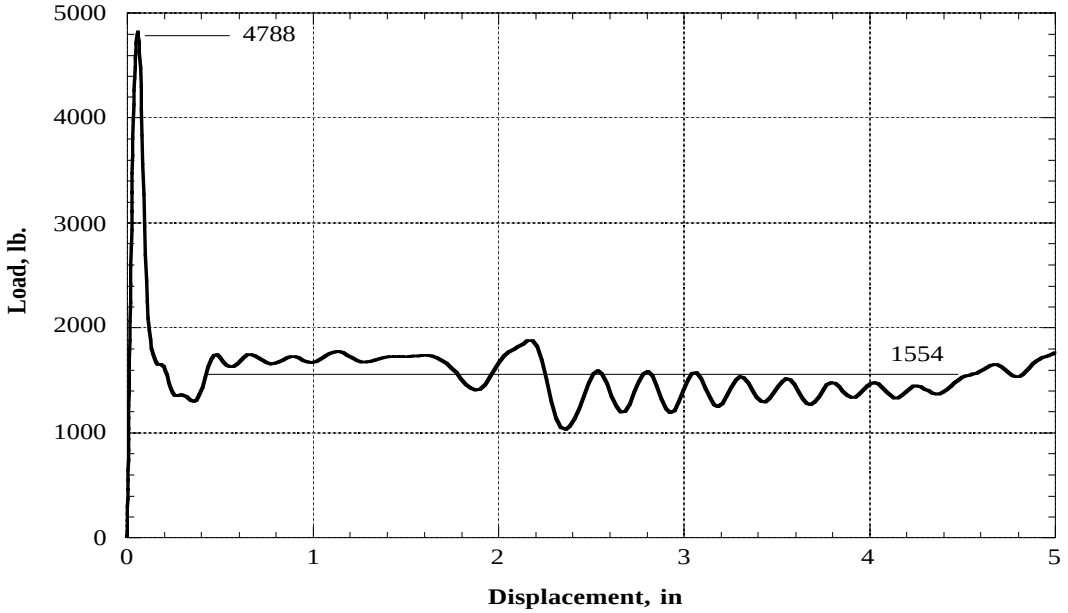

Fig.8 Dynamic Load/Displacement response of two (tandem) constrained-rings. The velocity at impact was approximately 16 ft/sec.

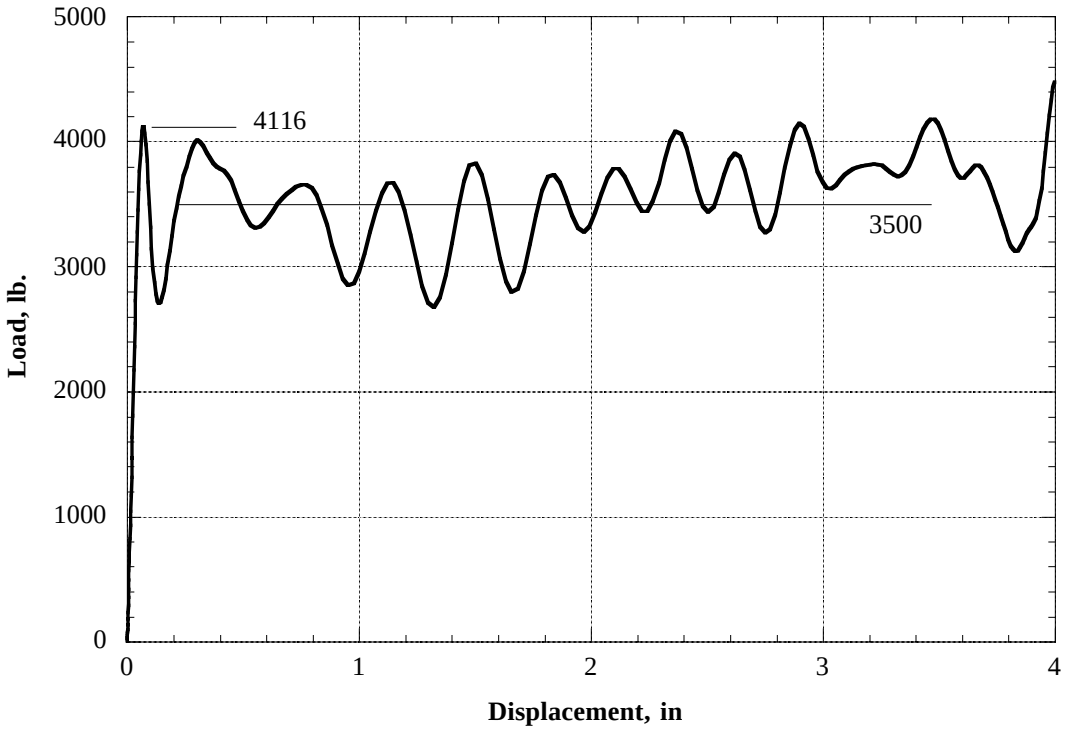

Fig.9 Dynamic Load/Displacement response of two (tandem) aluminum crush tubes. The velocity at impact was approximately 20 ft/sec.

Comparing the dynamic to the static response, an increase of 18.4% and 11.5% was observed for the crush initiation and the sustained crush load respectively. This small increase in crushing load was compatible with similar results found in the published literature, for example see reference [2], and thought to be acceptable for the present application.

FULL-SCALE ANALYSIS AND TESTING

Full scale tests were performed outdoors on a vertical 70 ft drop tower. For these tests, the seat was mounted on a custom build platform with the seat rails supported in a similar fashion to that in the actual plane. The full scale seat assembly is shown schematically in figure 10. All seat tests have been carried out with the seat positioned in the middle height position.

The drop tower consisted of a guided "π" shaped portal connected to an electric winch through a release hook. The specimen platform was suspended from the portal as shown in the photograph of figure 11. On release, from a predetermined height, the portal was decelerated independently of the specimen to allow for a desired input seat pulse to be produced. For all seat tests the input pulse was produced during the impact of the specimen platform with a mount of fine glass beads, contained in a steel box. The portal was decelerated to a complete stop, by two aluminum honeycomb columns, following the impact of the specimen platform with the glass beads. Eight channels of data were acquired at a rate of 10k samples/ sec. per channel, through an umbilical cord, into a personal computer. Accelerometer data were filtered at 250 Hz using a low pass "Chebyshev" filter routine. Typical data channels included; platform acceleration, occupant lumbar load, pelvis acceleration, etc. In addition to the transducer data, at least two video cameras were used in each test and, on one occasion two high speed film cameras were also used.

Two platform accelerometers were used in each test. The first with a maximum range of 25 G was used to measure the "free fall" acceleration, which due to drag and/or friction was slightly less than 1 G. On integration the data from this accelerometer produced the impact velocity. The second, with a maximum range of 750 G was used to determine the input pulse.

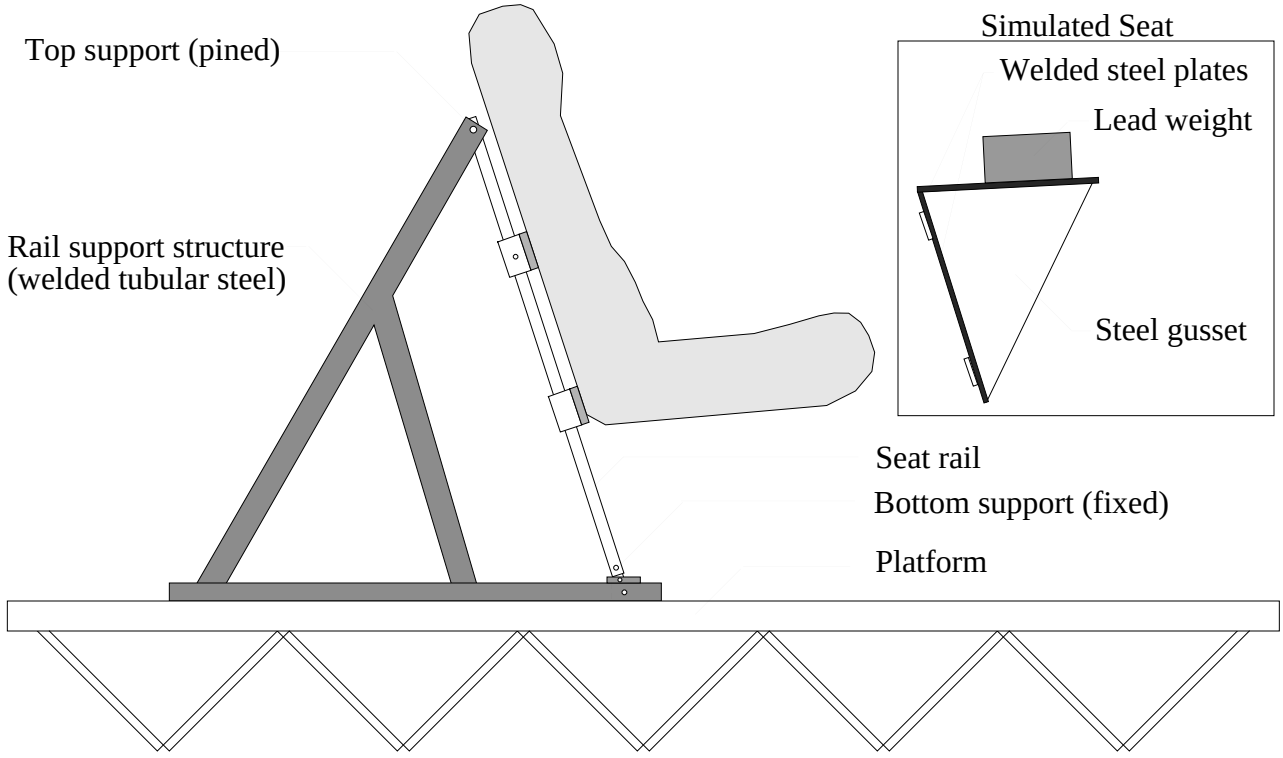

Fig. 10 Schematic of full-scale test assembly. Note that the top and bottom seat rail supports are equivalent the rail supports found in the aircraft.

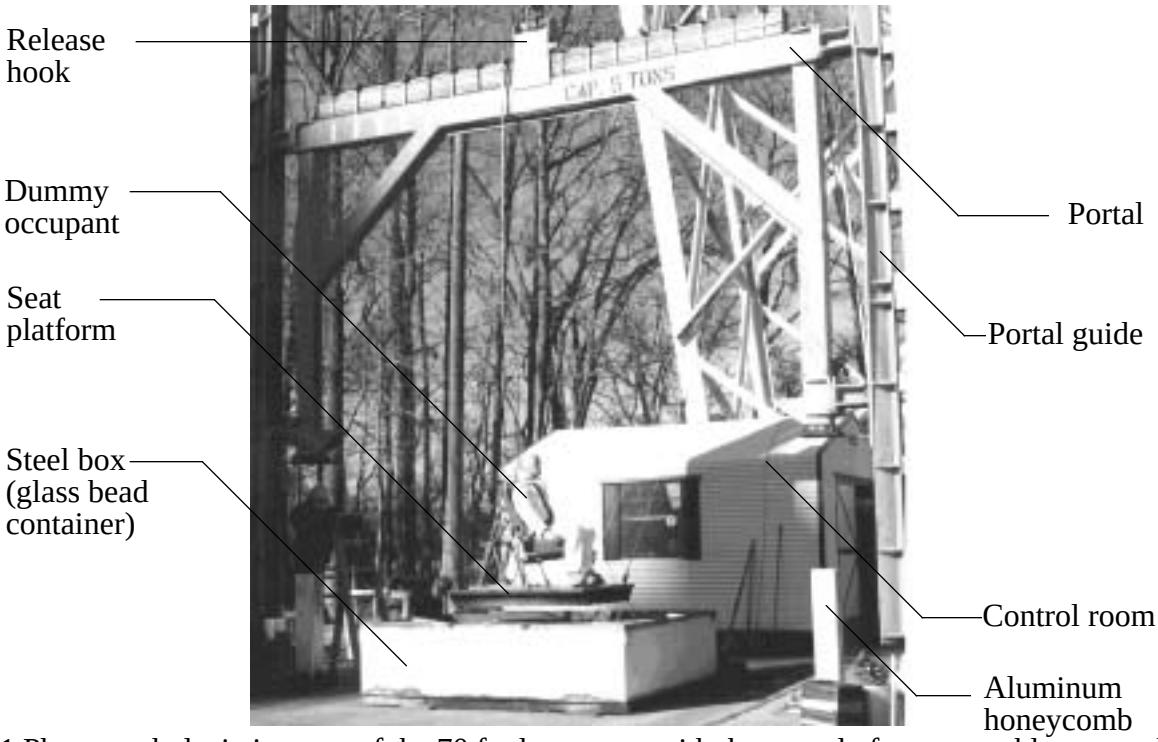

Fig. 11 Photograph depicting part of the 70 ft. drop tower with the seat platform assembly suspended by the portal prior to a full scale test.

In some preliminary tests the aircraft seat, shown in figure 10, was replaced by a custom-build simulated seat assembly, shown in the inset of figure 10. The simulated seat was designed to have similar weight distribution to that of the aircraft seat plus active occupant weight, and could accommodate the original seat brackets in the same way.

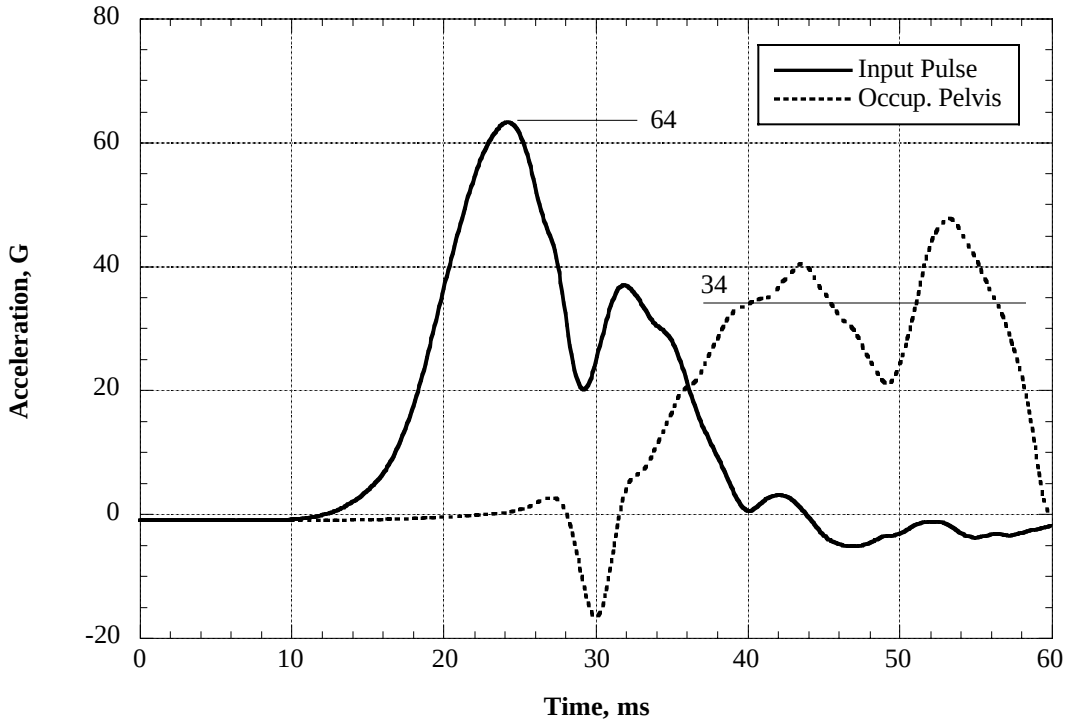

Fig.12 Crash acceleration/time responses for platform and occupant pelvis from first preliminary test. Vertical velocity at impact was 25.7 ft/sec.

The first full scale test was carried out on the original seat assembly at a relatively mild impact velocity of 25.7 ft/sec., in order to obtain reference occupant loads. The platform acceleration, from this test, is presented together with the occupant pelvis acceleration response in figure 12, and the occupant lumbar-load response in figure 13.

In these figures, accelerations corresponding to the gravity direction are shown negative and a compressive lumbar force is indicated by a negative sign. These conventions for acceleration and force are used throughout this report.

Figure 12 shows that, a significant percentage of the dynamic crash load is transmitted to the pelvis with an average level of 34 G for approximately 20 msec.. Such level of acceleration would normally lead to a fatality.

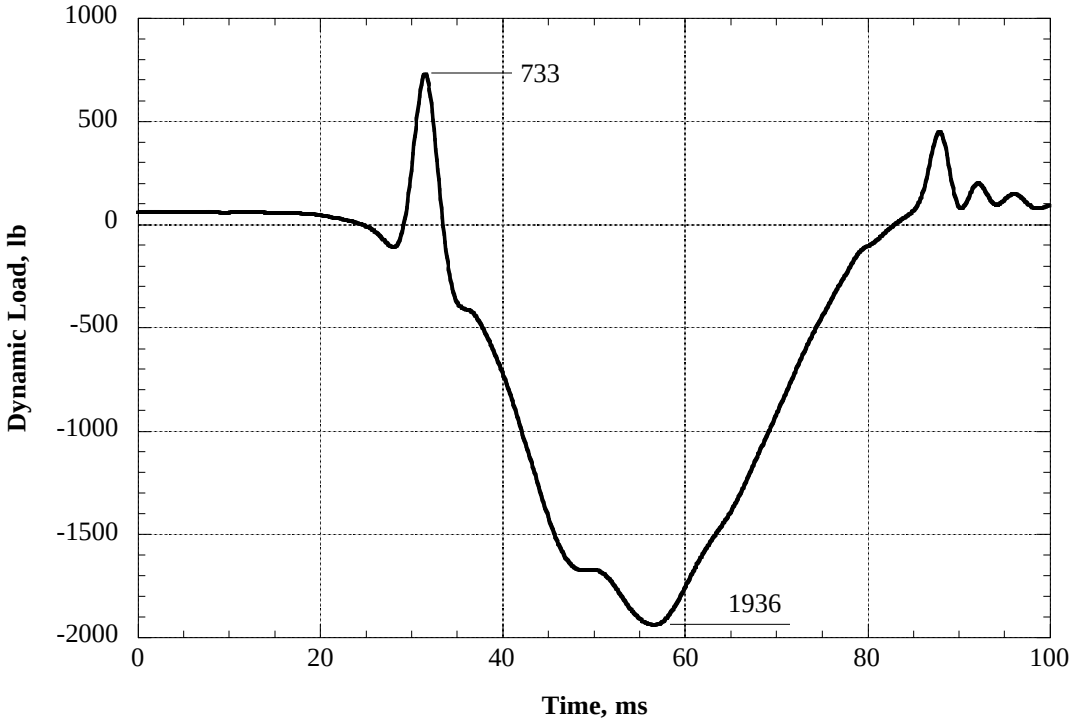

Fig. 13 Lumbar-load/time response for dummy occupant during first preliminary test. Vertical velocity at impact was 25.7 ft/sec.

A better measure of occupant survivability, however, can usually be obtained by measuring the lumbar loads with a load cell placed in-line with the spinal column. It is generally thought that the vertical crushing strength of the spinal column is greater than 1500 lb., reference [3]. Results from this test, figure 13, indicated that the limit of 1500 lb. was exceeded by nearly 30%, which could result in either severe injury or a fatality.

During the first test, the rear seat-pan frame member, which supports the stretched fabric was partly fractured (approximately 0.5” away from the weld points) and bent downwards. Moreover, fabric failure initiated at the rear/right corner of the seat pan. The damage areas are shown in figure 14.
The seat damage was repaired and subsequent preliminary full-scale tests were carried out using the simulated seat assembly until adequate stroking of the seat was achieved.

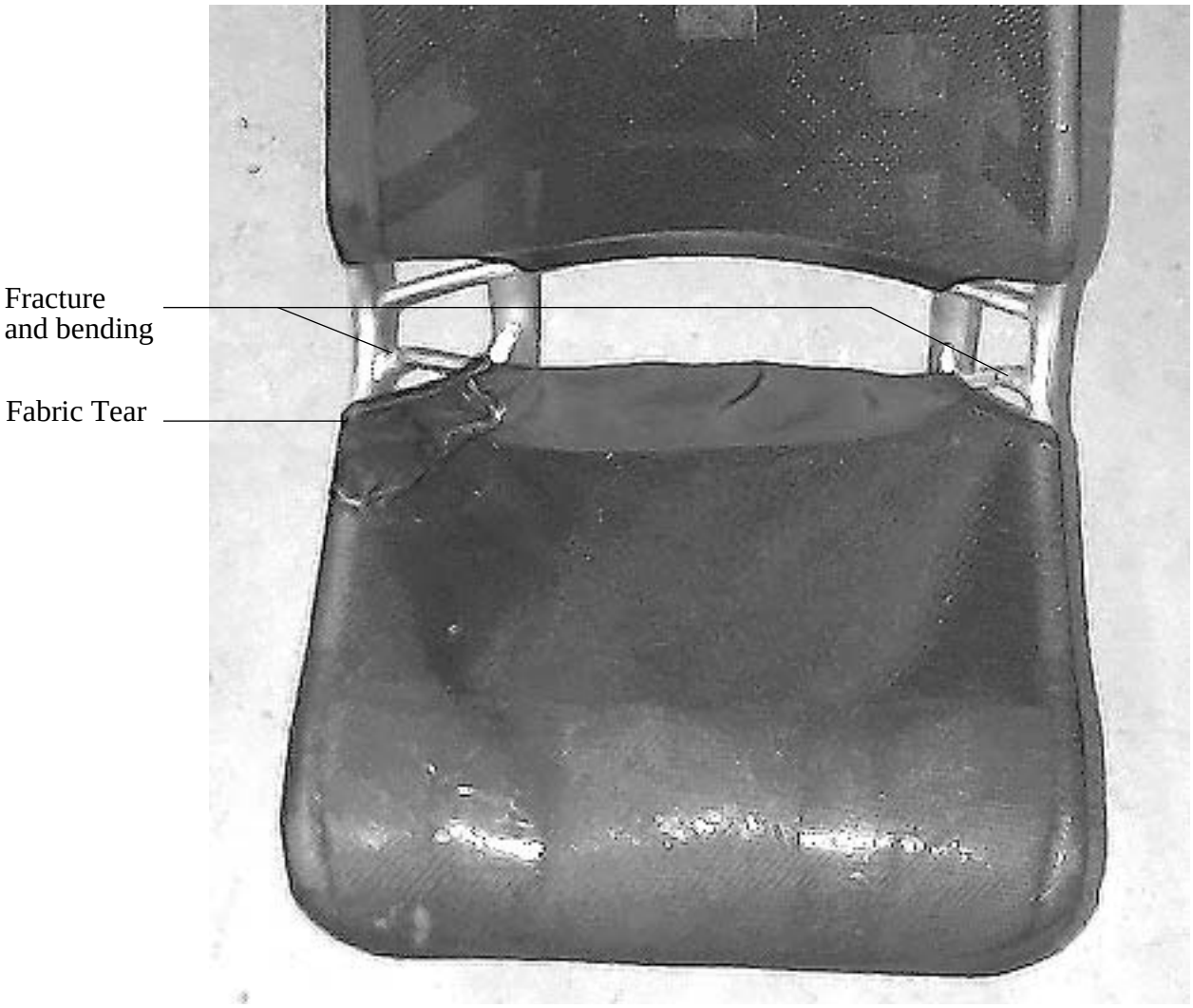

Fig. 14 Photograph of seat showing the damage in frame and fabric.

Several problems were highlighted during the first test but, by far, the most important one was the bending of the seat rails. At least 0.5" of residual deflection was observed at a point immediately below the bottom seat bracket. Clearly stroking of the seat could not take place unless bending of the seat rails was suppressed.

Bending loads, responsible for the rail deformations, were evaluate through a simple (statically determinate) model, shown in figure 15. Using static equilibrium, expressions were developed for the maximum bending stress as well as the magnitude of friction, at impending sliding, as a function of the rail angle θ. Note that under realistic crash conditions a large forward force will act on the seat rails as well as the vertical component. Therefore, the resultant vector of the dynamic seat load will not be vertical. Since this is equivalent to rotating the rail relative to a fixed vertical force, the effect of the resultant load, other than vertical, can be studied by varying the rail angle θ. Note further that, with the presence of any forward seat-load component, the magnitude of the resultant will always be greater than the vertical component used here for the design of the energy absorbers. Therefore, the effect of the rail angle relative to the load vector, can only be used for observing trends and NOT for predicting realistic crash loads.

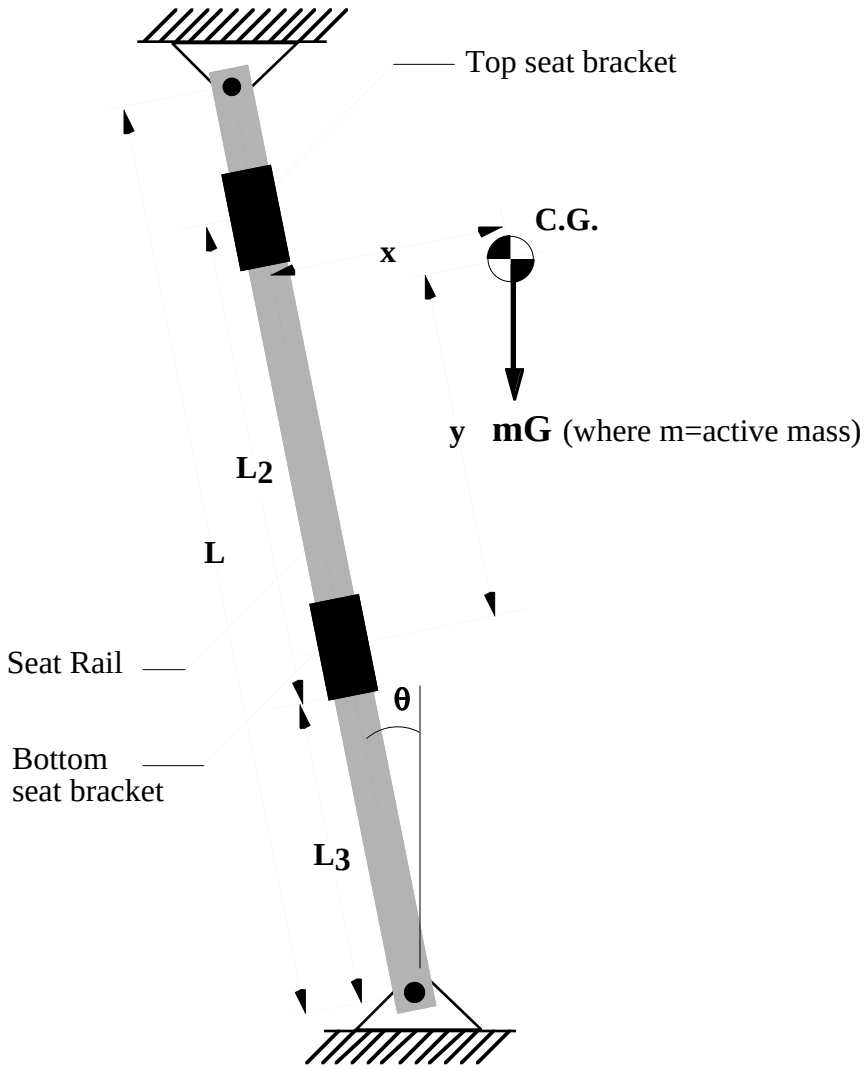

Fig. 15 Schematic of the statically determinate seat rail used in the evaluation of maximum bending stresses and friction.

The assumptions made in this simple approach are:

(a) the problem is a two dimensional one, no out of plane loads act on the seat, this means that the seat loads are reacted equally by each rail,
(b) the C.G. position relative to the bottom bracket remains uniform throughout the crash event,
(c) the transverse reactions transferred to the rails by the brackets are point loads, this in effect means that the length of each seat bracket is neglected,
(d) there is no moment acting at the C.G., and
(e) top and bottom rail supports are pure pin joints (support zero moment).

The C.G. position was measured with the dummy occupant (minus the legs) strapped in the aircraft seat. The x-y co-ordinates were found to be approximately 7” and 14” respectively. Other input values include; L=29”, L_2=13”, rail wall thickness = 0.106”, rail outer diameter =1.04”, and active mass = 158 lb. Another not very well defined input, needed for this analysis, is the coefficient of friction. This value for impending motion could, in practice, be anything between 0.16 (for lubricated steel on steel) to 0.8 (dry steel on steel).

Typical maximum stress results from this study are shown in figure 16.

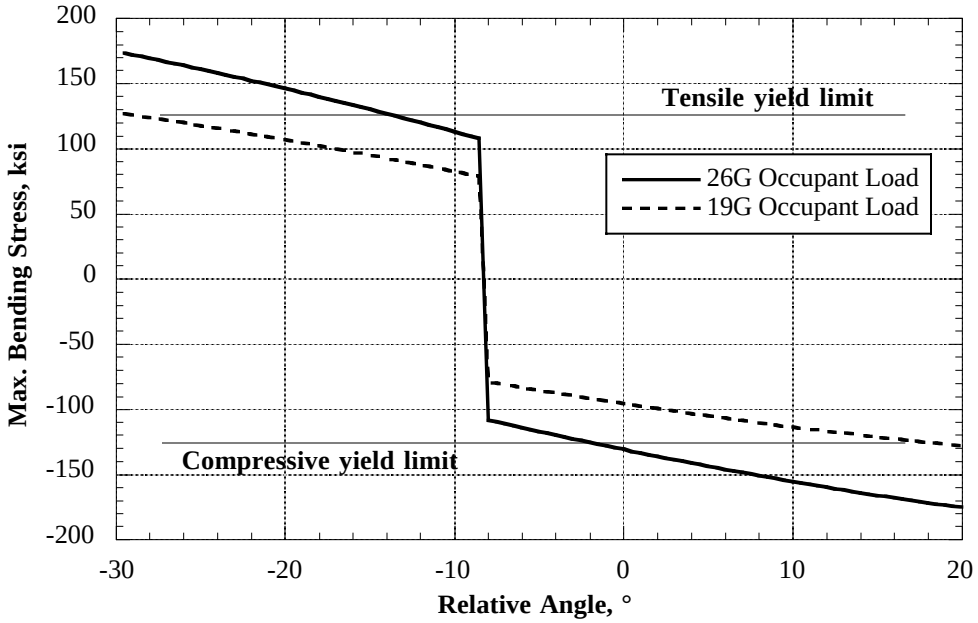

Fig.16 Maximum bending stress as a function of the relative angle between the seat rails and the dynamic seat load. Positive bending stress indicates center of curvature towards the rear of the plane.

The tensile yield limits, shown in figure 16, represent measured values from three-point-bend tests carried out on aircraft quality 4130 tube stock. The actual designation of the material used in the bend tests is: MIL-T-67367, condition N, 0.083" wall and 1.00" outer diameter.

Figure 16 shows that the maximum stress in the rails is least severe when the rail angle is approximately -8°. In other words, a small forward dynamic component of load would alleviate some of the rail bending load. Moreover it shows that, with the rails at 20° to the vertical (present full-scale test condition) impending plastic bending will occur when the dynamic seat-load exceeds 19G. This result was actually confirmed during the first full scale test. However, it has to be pointed out that had stroking of the seat occurred bending of the rails would be suppressed since the effect of a moving transverse load (rail reaction) would be equivalent to a distributed load.

Note that, due to the static nature of the solution used, the bending stress is not a function of the friction coefficient. However, the desired crushing load is. In figures 17 and 18 the required crush load (per rail) was calculated as a function of the relative rail angle for two hypothetical dynamic seat loads, 19G and 26G. The minimum expected static (impending motion) coefficient of friction, 0.16, was used to derive the trends shown in figure 17, and the maximum, of 0.8, was used for figure 18.

The influence of the coefficient of friction on the required crashing load can be seen by comparing figure 17 to figure 18. For example, in the case of 26G design load limit and θ=20°, the difference in the required crushing load is nearly 50%. Note also that, for as long as the coefficient of friction is approximately equal to 0.16, the required crushing load value (per energy absorber) falls within the preliminary design load (1650±250 lb.) for a large range of rail angles.

Clearly, bending of the rails and the magnitude of the frictional resistance became the primary hurdle to overcome before stroking of the seat could be achieved and, hence, crash energy could be attenuated.

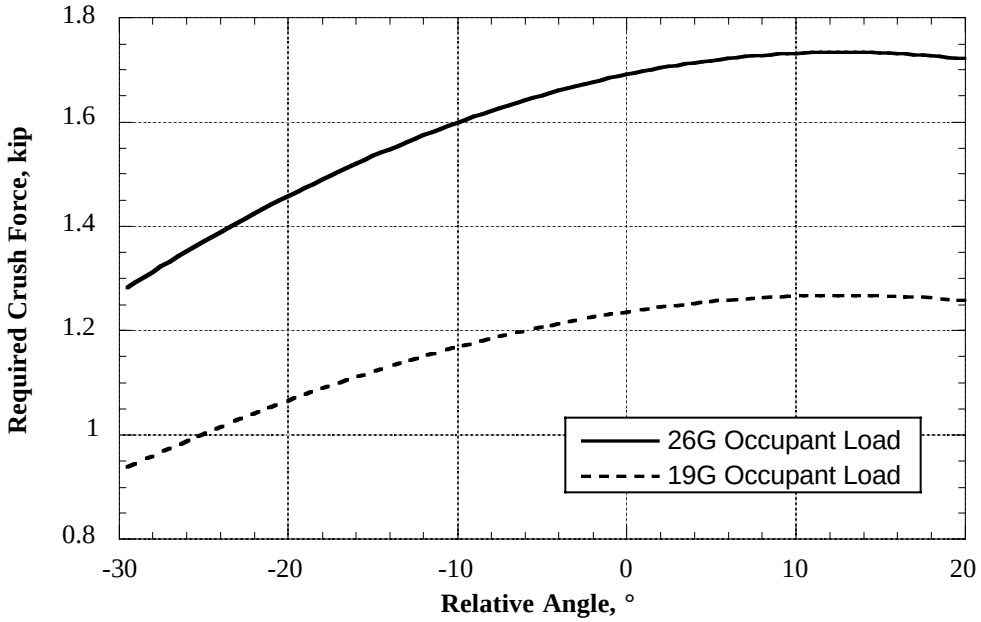

Fig.17 Required crush load (per rail) as a function of the rail angle. The minimum expected value of the static coefficient of friction (0.16) was used.

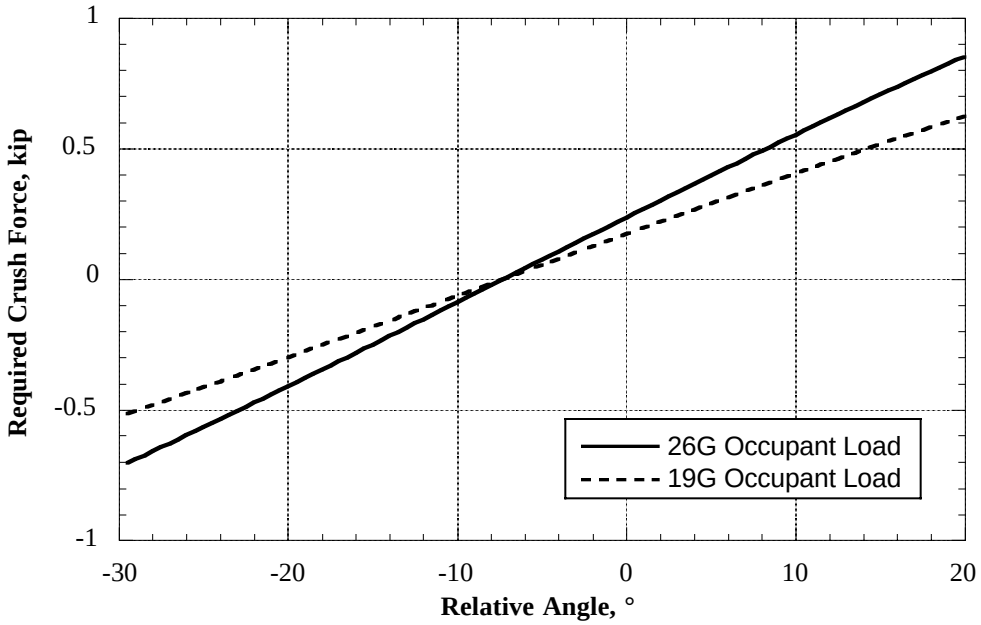

Fig.18 Required crush load (per rail) as a function of the rail angle. The maximum expected value of the static coefficient of friction (0.8) was used.

The problem of rail bending was investigated first. Three possible options were studied separately and in combination. These options were;

(a) minimize the effective rail length by lowering the top rail support by 6". This would still allow enough room for seat height adjustments,
(b) replace the original seat rails with same O.D. but thicker wall steel tubing. Analysis indicated that a 0.25" wall thickness would be adequate, and

(c) reinforce the original seat rails with unidirectional graphite, molded and cured in place inside the tubular rail to add bending stiffness in the area of maximum stress. To accommodate the full range of height adjustment a total of 8" of rail length had to be reinforced which resulted in a 6% increase in rail weight, and at least 30% increase in the transverse load capacity.

Full scale testing using the simulated seat assembly indicated that any of the above methods was adequate in suppressing seat-rail yielding. However, seat binding could not be eliminated. As a result, the bottom seat bracket, where binding occurred, had to be redesigned. The original and redesigned bottom seat brackets are shown in figure 19. The redesigned seat bracket was made of mild steel using a standard 1/4" thick angle section. The new bracket, in addition to eliminating binding, offered several advantages over the original design, two of which are;

(a) simple design could eliminate several fabrication steps. Could also be made lighter by using 1/8" thick 4130 steel instead of 1/4" thick mild steel and,
(b) offered extra clearance with the potential of accommodating a longer (up-to 10.5" long) energy absorber between the top and bottom seat bracket.

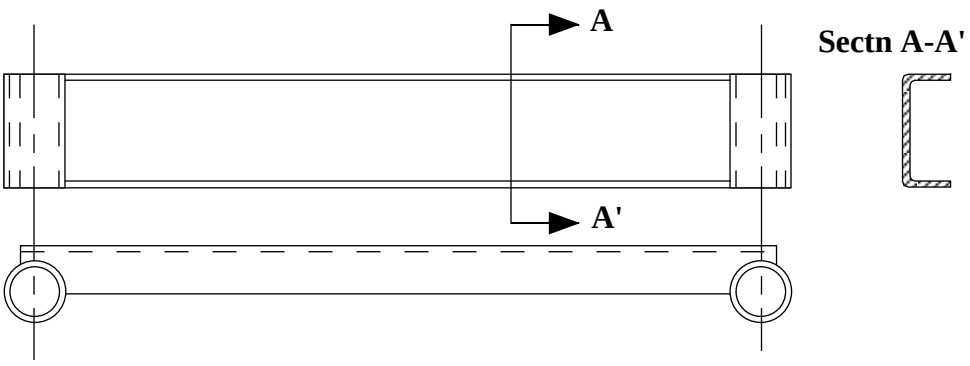

(a) Original Bottom Seat Bracket

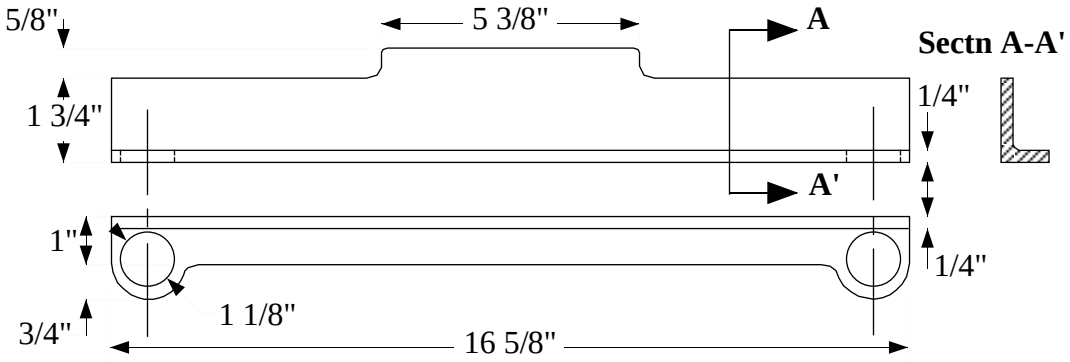

(b) Redesigned Bottom Seat Bracket

Fig.19 Original and redesigned bottom seat bracket. The mounting holes are not shown.

Two preliminary full-scale tests (test 7 and test 8) were carried out using the simulated seat fixture to investigate the performance of the redesigned seat bracket. In test 7 the new seat bracket was tested in combination with a set of stiffened rails. In test 8 the bracket was tested in combination with a set of rails similar to the original seat rails. Both tests were successful: stroking of the seat occurred and the dynamic seat load was attenuated from 76G to an average of 21G as shown in figure 20. This figure shows that, on rebound, the seat stroked upwards with the seat load being limited to approximately 6G.

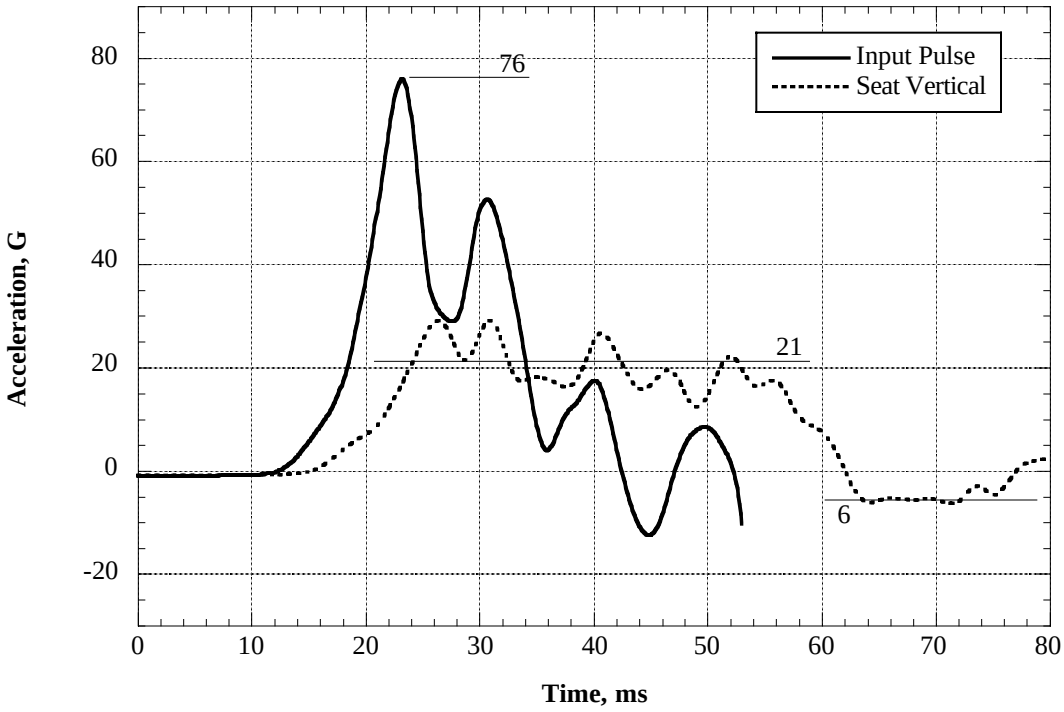

Fig.20 Crash acceleration/time responses for platform and simulated seat equipped with a redesigned bottom seat bracket. Seat rails similar to the original ones were used. The vertical velocity at impact was 29.5 ft/sec.

Thus, the objective of providing energy absorption during both the compressive and the tensile stroke of the seat was clearly met.

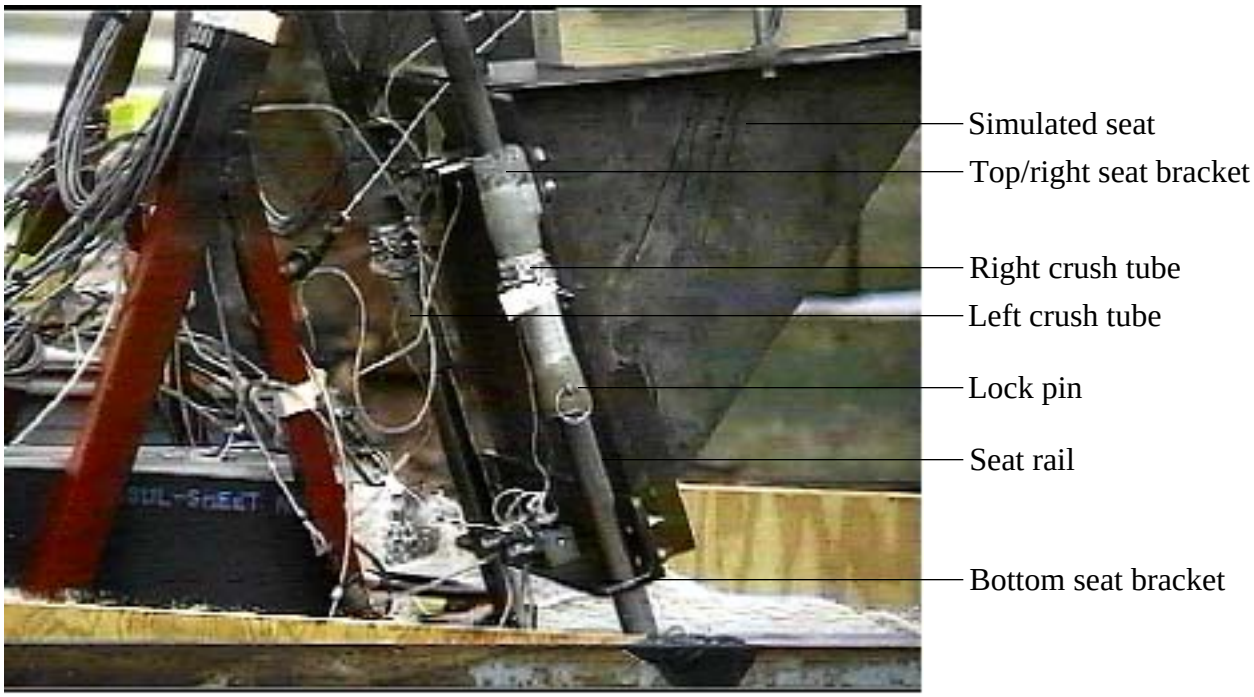

Fig.21 Photograph of simulated seat assembly after a crash test at 29.5 ft/sec. impact velocity.

A photograph of the simulated seat, after the test, is shown in figure 21. At least 3” of residual crush stroke is evident in this photograph.

Following the success of the redesigned seat bracket on the simulated seat, a full scale test (test 9) with the actual aircraft seat and a dummy occupant was performed. In this test the redesigned bottom bracket was used in combination with a set of original seat rails.

The test was carried out at a maximum velocity of 29.5 ft/sec. (same as test 8). Acceleration responses for the input pulse and the occupant pelvis are shown in figure 22. While the input pulse was attenuated to an average of 29G at the occupant pelvis, the residual seat stroke was only 0.5”, figure 23, as opposed to 3” for the simulated seat. Clearly, there must be a difference in the way energy is dissipated between the two set-ups. Differences can be attributed two at least two possible causes:

(a) as opposed to the rigid simulated seat, some crash energy is absorbed by the actual aircraft seat through frame deformation and fracturing as well as fabric deformation and tearing. In fact, the actual seat allows the occupant to sink in approximately 3”, or more, before bottoming out occurs,
(b) as opposed to the simulated seat, the C.G. position of the actual seat plus occupant does NOT remain uniform, with respect to the bottom seat bracket, during a crash. This could in practice aggravate the binding problem and delay, or even inhibit, stroking of the seat.

The speculation that energy is absorbed by the seat can be justified by observing the damage in the seat. However, the second speculated cause, or at least its effect on the seat stroke, is not readily clear. One way to assess the possibility of additional frictional forces is to compare the dynamic load response along the rail direction for the rigid-simulated seat and the actual aircraft seat.

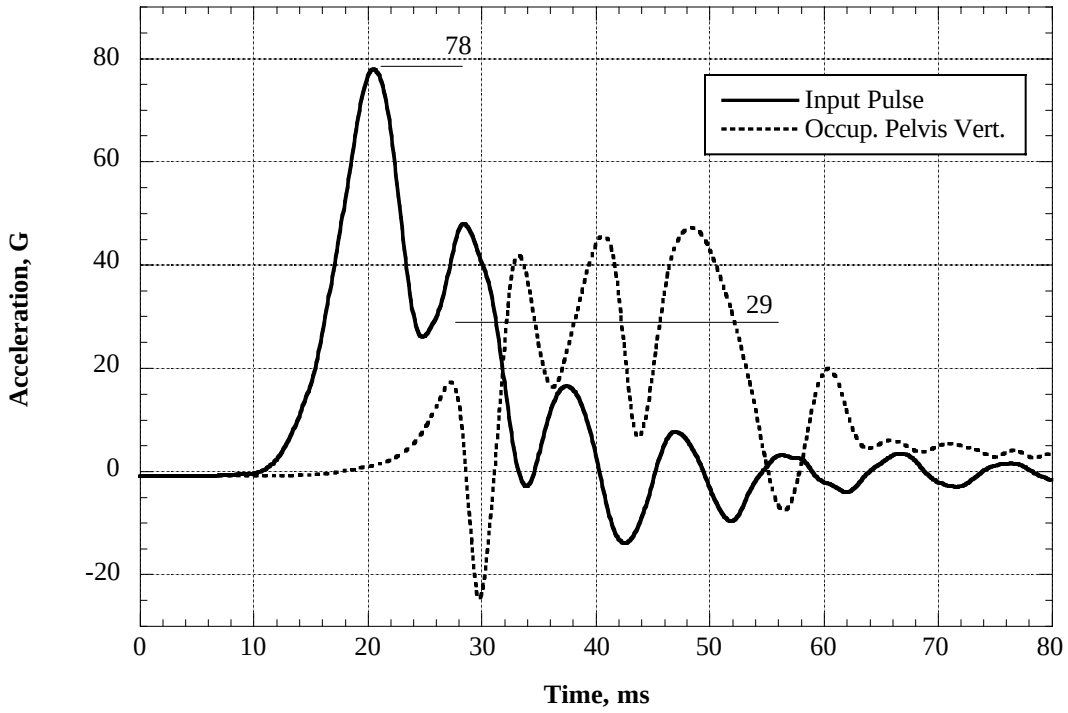

Fig.22 Crash acceleration/time responses for platform and occupant pelvis with the redesigned bottom seat bracket mounted on actual aircraft seat . The original seat rails were used. The vertical velocity at impact was 29.5 ft/sec.

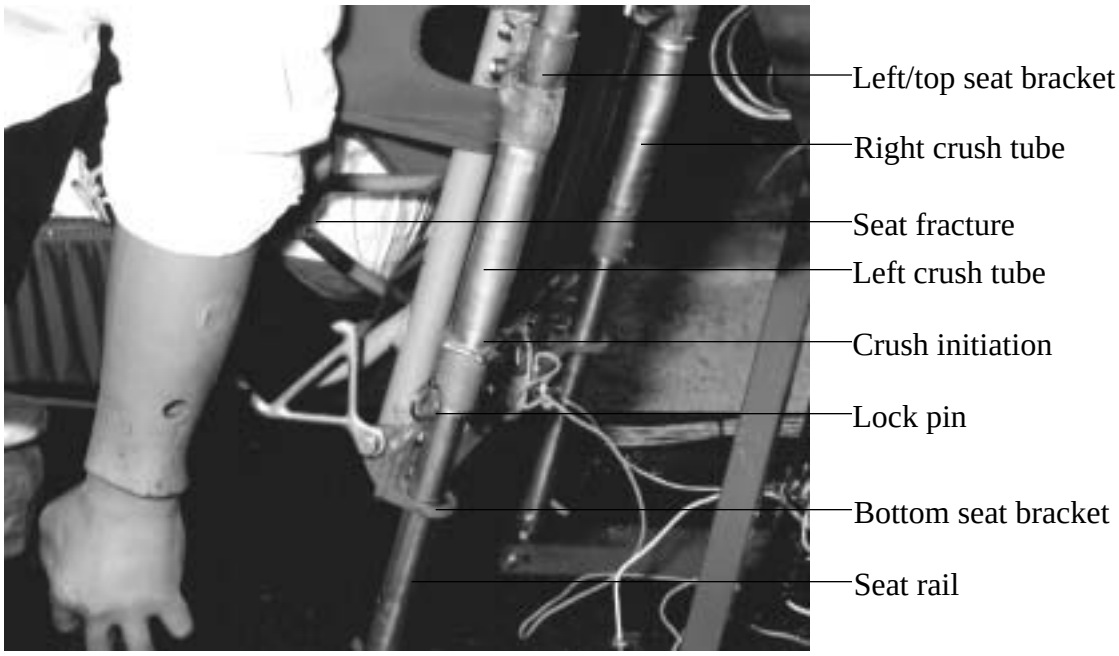

Fig. 23 Photograph of aircraft seat assembly after a full scale test, showing a relatively small amount of crushing in aluminum energy absorbers. The vertical velocity at impact was 29.5 ft/sec.

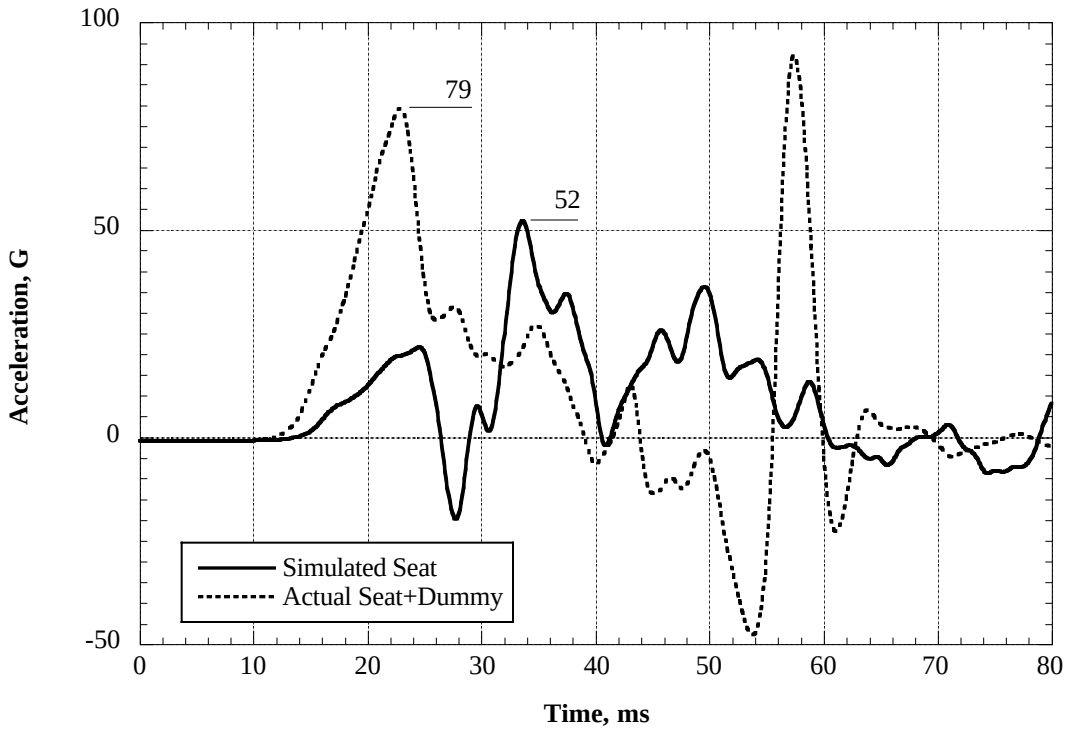

Fig.24 Acceleration responses for the simulated seat and actual aircraft seat, measured along the rail direction at the bottom bracket position.

Since similar crush tubes have been used in both tests (test 8 and test 9) and since the active mass for both tests was equivalent, crushing should have initiated at approximately the same G level. However, the accelerations along the seat rail direction, shown in figure 24, indicate that the crash initiation load for the actual seat is 52% greater than that of the simulated seat. A very plausible explanation for this is additional friction along the rail direction.

In order to counter the effect of greater frictional force on the crush stroke of the actual aircraft seat, methods of attenuating the crush initiation load of the aluminum tubes through a trigger mechanism were considered. The objective was to modify the tubes so that the crush initiation load would actually be lower than the sustained crush load. A minimum limit for the crush initiation load was thought to be necessary to ensure that stroking of the seat could not take place during severe flying maneuvers and/or hard landings. The lower limit for the crush initiation load was set to correspond to the range of 10G to 12G. For the 158 lb. active occupant plus seat mass this translated to a range of 740 lb. to 890 lb., along the rail direction.

To attenuate the crash initiation load a trigger mechanism was introduced in the center of the crush tube. This consisted of a 1/16" deep waste (wrinkle) around the tube's perimeter. The waste was plastically introduced into the tube with a pipe cutting tool equipped with an 1/8" thick wheel. Two methods have been examined both of which included annealing of the tube to counteract the effect of work hardening, caused by the introduction of the indentation. In the first case the waste was introduced after the tube was annealed and, in the second case the waste was introduced before the tube was annealed. The same heat treatment, shown in figure 25, was followed in both cases.

The static crushing characteristics of the wasted tubes are compared against that of the plain tube in figure 26. Results show that the annealed specimens exhibited a similar sustained crush load, which was approximately 30% lower than that of the plain tube. The crush initiation load was also attenuated, however, the order in which the wasting was introduced was very important, with as much as 70% reduction observed in the specimen which was wasted first. The specimen which was wasted after it was annealed showed a 50% reduction in the crush initiation load. This specimen type, with a crush initiation load of 840 lb., was selected and subsequently installed on the seat for full scale testing.

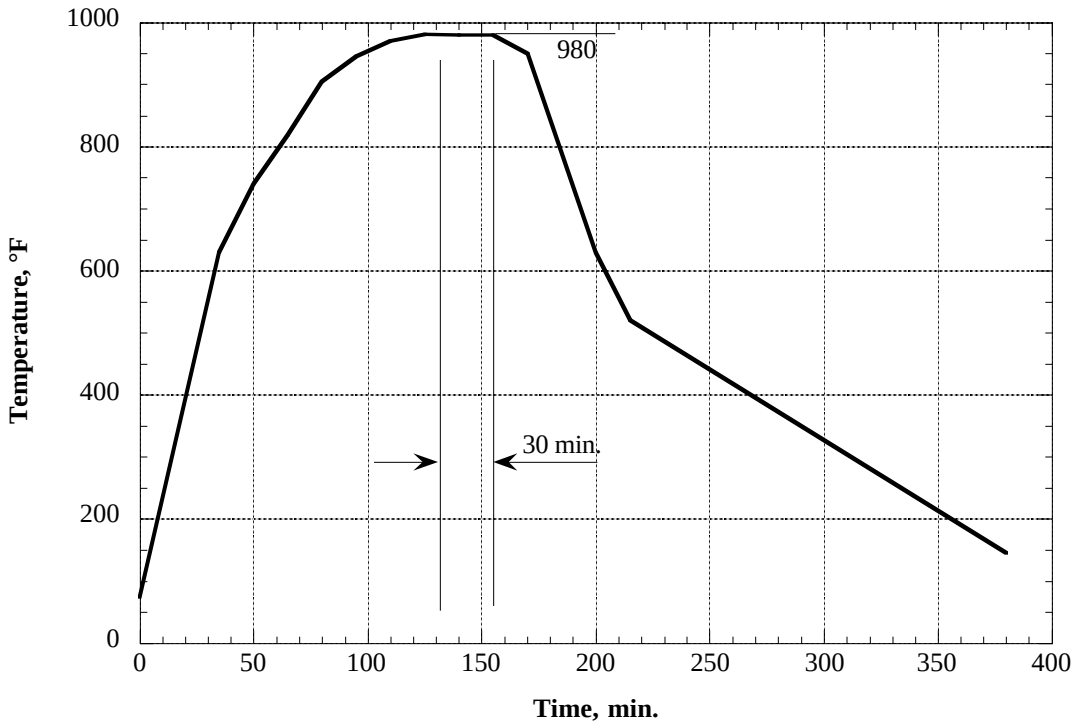

Fig.25 Heat treatment curve used during the annealing of the aluminum crush tubes.

Following repair of the seat, for the second time, and installation of the modified crush tubes, a final full-scale seat test (test 10) was performed with a velocity at impact of 32.5 ft./sec. This test was successful, producing a seat stroke in excess of 3". The crushing sequence is shown in the photographs of figure 27. The trigger mechanism, in the center of the crush tube, is evident in the first photograph of figure 27.

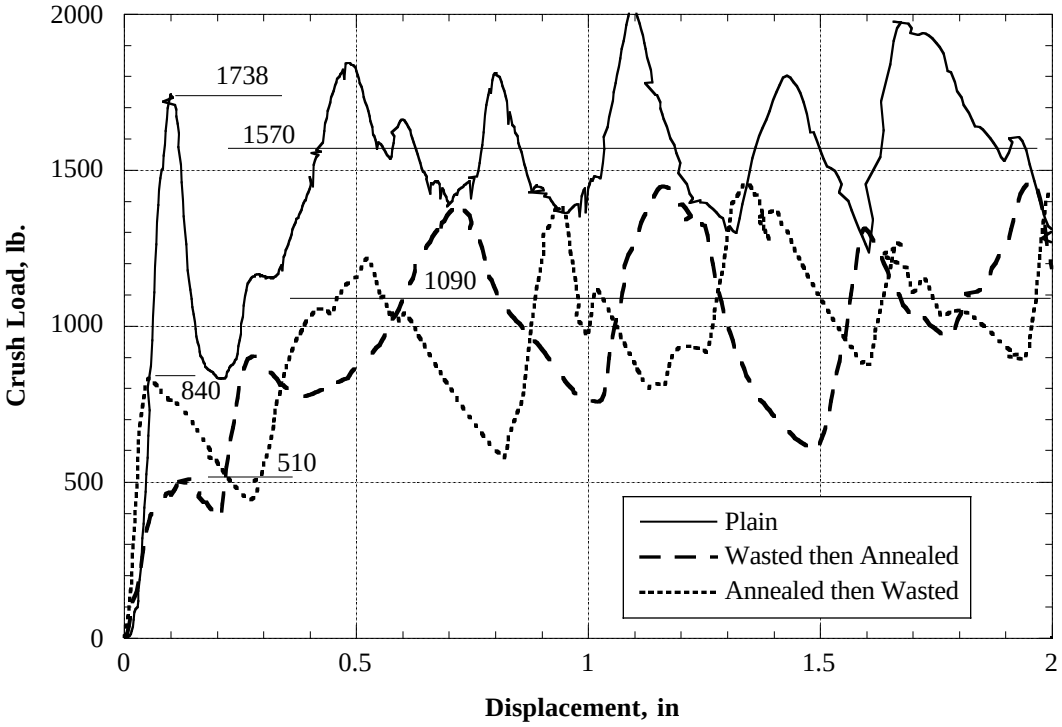

Fig.26 Static crush performance of plain and wasted aluminum tubes.

(a) Before impact (t=0) (b) t=33.3 msec. (c) t=66.6 msec. (d) t=100 msec.

Fig. 27 Photographs of aircraft seat showing the sequence of crushing of right crush-tube.

The acceleration time response of the occupant pelvis and input pulse from test 10 are shown in figure 28. Despite the fact that this final test was the most severe of all full scale tests, the average pelvis acceleration was nearly 40% less than that of test 9, and nearly 50% less than that of test 1, (figures 24 & 12).

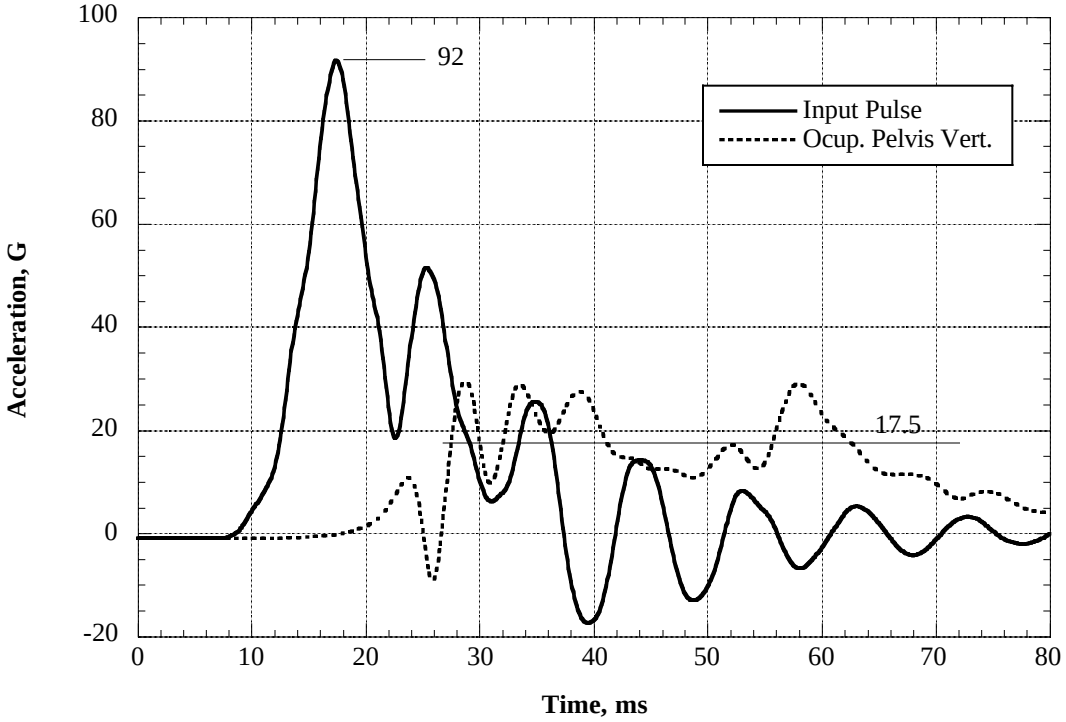

Fig.28 Crash acceleration/time responses for platform and occupant pelvis for the modified crush tube case. The original seat rails were used. The vertical velocity at impact was 32.5 ft/sec.

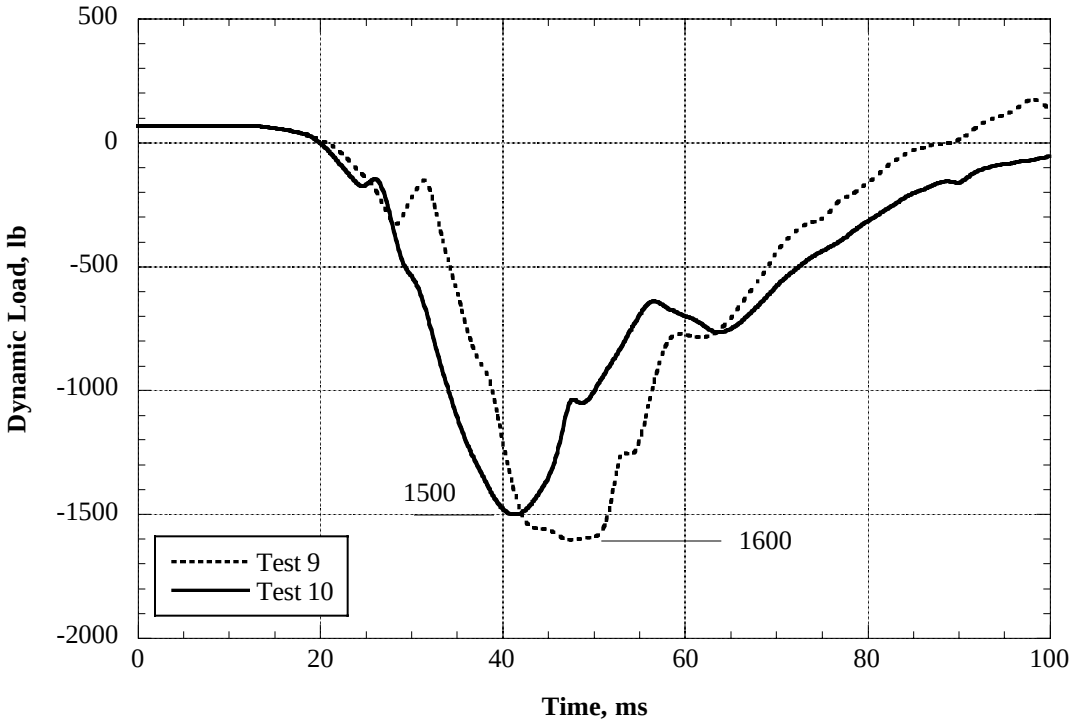

Fig.29 Occupant lumbar loads for tests 9 & 10. The velocities at impact were 29.5 and 32.5 ft./sec. respectively.

Furthermore, figure 29 shows that the maximum occupant lumbar load in test 10 was limited to 1500 lb. as opposed to 1600 lb. for test 9, thus resulting in what would be considered a survivable crash. The lumbar load attenuation between the first and the last test was at least 22.5% despite the fact that the seat energy at impact was nearly 60% greater.

CONCLUSIONS

An aircraft seat was retrofitted with a cost effective energy absorbing system and tested on a vertical drop tower to assess the performance of the system under purely vertical impact conditions. The input pulse generated at an impact velocity of 32.5 ft./sec. had a magnitude of 92 G and a total duration of approximately 20 msec.

Two energy absorbing concepts have been studied and one was chosen for a full-scale test demonstration. The chosen concept consisted of two thin wall aluminum tubes which absorbed energy by crushing. The crush initiation was regulated by the introduction of a trigger mechanism in the form of a hoop-wrinkle in the center of each tube.

It has been shown that the pelvis accelerations of a dummy occupant seated in the retrofitted seat, impacting at 32.5 ft/sec. were attenuated to an average level of 17.5 G with a corresponding maximum lumbar load of 1500 lb. In contrast, when the same dummy occupant was seated in the original seat, following a relatively mild impact velocity of 25.7 ft./sec., the average pelvis acceleration was 34 G and the corresponding maximum lumbar load was 1936 lb. In other words, the energy absorbing system provided a 48% attenuation for the average pelvic acceleration and 22.5% attenuation in the lumbar load while the total energy at impact was nearly 60% greater. This improvement was achieved with an increase in the total seat weight of less than 3%.

RECOMMENDATIONS

While it has been shown that the energy absorbing seat system will provide adequate crash energy management for vertical impacts, it is believed that, in addition to airbags, further modifications may be necessary to ensure adequate stroking of the seat under more complex and/or severe crash situations. Some of the possible improvements include:

(a) Occupant loads could be attenuated further by modifying the top bracket as shown in figure 30 . This not only will provide a simpler fabrication process, but also will minimize further the possibility of binding, it will allow for a longer crush tube and, could provide a better way to couple the aluminum tube using fiber reinforcement wrapped around the tube and through the slot, shown in figure 30.

(b) Seat rail reinforcement, while not necessary for vertical impacts, maybe advantageous to have in more realistic crash cases where a large forward acceleration component occurs. Seat rail reinforcement through internal graphite reinforcement (see figure 31 for fabrication process) was proven to improve the bending stiffness and strength of the rails without a significant weight penalty. A more cost effective alternative is to replace the original rails with new thicker-wall rails. However, this will result in a significant weight penalty. In any case, alteration of the seat rails has to be accompanied by an analysis to verify that the seat rail attachment points can support the crash loads.

(c) Seat replacement. While the original aircraft seat appears to be designed well and provides some vertical crash protection to the occupant, it does not offer any advantage when used in combination with an energy absorbing system, such as the proposed crush tubes. One major disadvantage, brought out by the present tests, is the sinking of the occupant into the seat pan. This in effect renders the shoulder belt ineffective, particularly during a realistic crash event, where forward occupant restraint will be vital. The seat could be replaced by a one-piece molded composite of hybrid glass/graphite materials to provide a light weight and stiff seat. Moreover such construction could integrate the seat brackets to eliminate extra fabrication steps, therefore reducing overall cost. Rate sensitive foam cushions should be used in the seat pan for comfort and to minimize relative motion between occupant and seat during a crash. In such a seat design, the same seat belt arrangement, used in the present aircraft seat, will be made much more efficient. Another

advantage would be a shallower seat pan which in effect will allow for as much as 4 extra inches of crush space, thus making the crush tube design even more desirable and effective.

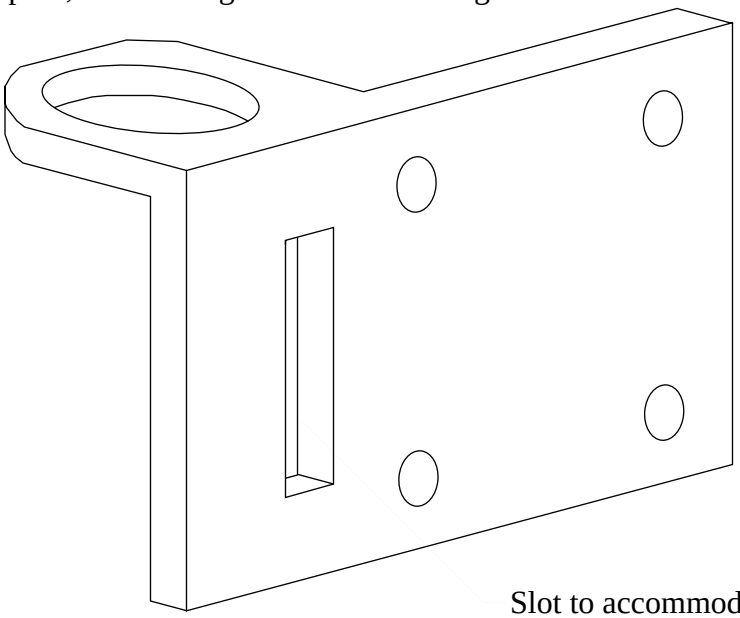

Fig. 30 Suggested top seat-bracket fabricated from standard angle-section does not require welding, and provides clearance for a longer crush tube. The right bracket is shown here in the upright position.

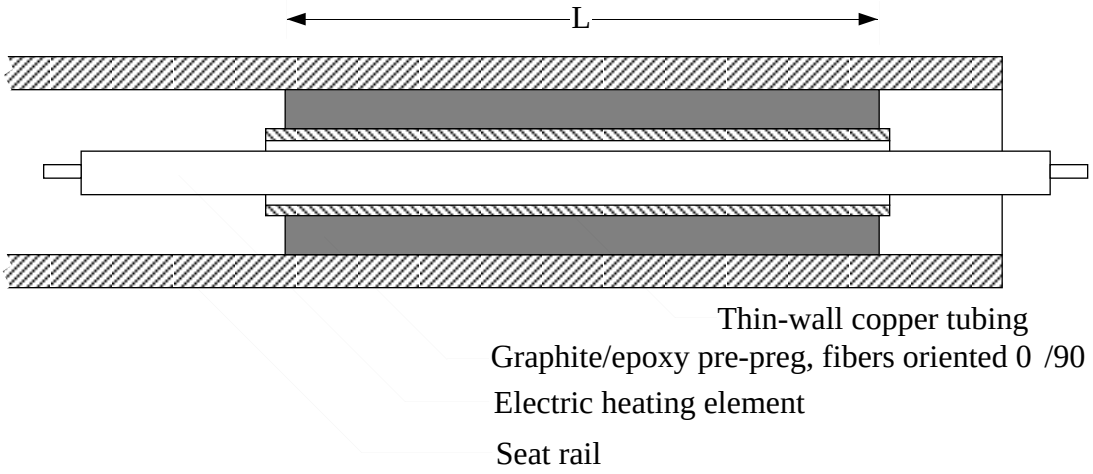

Fig. 31 Schematic of set-up used for the molding and curing of internal graphite reinforcement. The length, L, of the reinforcement was approximately 8" with its center located around the bottom seat bracket position.

REFERENCES

[1] Alexander J.M., "An Approximate Analysis of the Collapse of Thin Cylindrical Shells Under Axial Loading", Quarterly Journal of Mechanics and Applied Mathematics, 13, 10-15, 1960.

[2] Jones N., "Structural Impact", Section 9.3; "Dynamic Axial Crushing of a Circular Tube", Cambridge University Press, 1989.

[3] Eiband, A. M., Human Tolerance to Rapidly Applied Accelerations: A Summary of the Literature", NASA Memorandum 5-19-59E, June 1959.

REPORT DOCUMENTATION PAGE

Form Approved
OMB No. 0704-0188

1. REPORT DATE *(DD-MM-YYYY)*	2. REPORT TYPE	3. DATES COVERED *(From - To)*
12-2002	Contractor Report	

4. TITLE AND SUBTITLE
Energy Absorbing Seat System for an Agricultural Aircraft

5a. CONTRACT NUMBER
NAS1-96014

5b. GRANT NUMBER

5c. PROGRAM ELEMENT NUMBER

6. AUTHOR(S)
Kellas, Sotiris

5d. PROJECT NUMBER

5e. TASK NUMBER

5f. WORK UNIT NUMBER
728-50-10-01

7. PERFORMING ORGANIZATION NAME(S) AND ADDRESS(ES)
NASA Langley Research Center
Hampton, VA 23681-2199

8. PERFORMING ORGANIZATION REPORT NUMBER

9. SPONSORING/MONITORING AGENCY NAME(S) AND ADDRESS(ES)
National Aeronautics and Space Administration
Washington, DC 20546-0001

10. SPONSOR/MONITOR'S ACRONYM(S)
NASA

11. SPONSOR/MONITOR'S REPORT NUMBER(S)
NASA/CR-2002-212132

12. DISTRIBUTION/AVAILABILITY STATEMENT
Unclassified - Unlimited
Subject Category: 05
Availability: NASA CASI (301) 621-0390 Distribution: Standard

13. SUPPLEMENTARY NOTES
An electronic version can be found at http://techreports.larc.nasa.gov/ltrs/ or http://techreports.larc.nasa.gov/cgi-bin/NTRS
Langley Technical Monitor: Lisa E. Jones

14. ABSTRACT

A task was initiated to improve the energy absorption capability of an existing aircraft seat through cost-effective retrofitting, while keeping seat-weight increase to a minimum. This task was undertaken as an extension of NASA ongoing safety research and commitment to general aviation customer needs. Only vertical crash scenarios have been considered in this task which required the energy absorbing system to protect the seat occupant in a range of crash speeds up to 31 ft/sec. It was anticipated that, the forward and/or side crash accelerations could be attenuated with the aid of airbags, the technology of which is currently available in automobiles and military helicopters. Steps which were followed include, preliminary crush load determination, conceptual design of cost effective energy absorbers, fabrication and testing (static and dynamic) of energy absorbers, system analysis, design and fabrication of dummy seat/rail assembly, dynamic testing of dummy seat/rail assembly, and finally, testing of actual modified seat system with a dummy occupant. A total of ten full scale tests have been performed including three of the actual aircraft seat. Results from full-scale tests indicated that occupant loads were attenuated successfully to survivable levels.

15. SUBJECT TERMS
Crash-worthiness; Survivability; Energy-absorption; and Crushing

16. SECURITY CLASSIFICATION OF:			17. LIMITATION OF ABSTRACT	18. NUMBER OF PAGES	19a. NAME OF RESPONSIBLE PERSON
a. REPORT	b. ABSTRACT	c. THIS PAGE			STI Help Desk (email: help@sti.nasa.gov)
					19b. TELEPHONE NUMBER *(Include area code)*
U	U	U	UU	31	(301) 621-0390